Research Square

Preprints are preliminary reports that have not undergone peer review.
They should not be considered conclusive, used to inform clinical practice,
or referenced by the media as validated information.

Oral Nanoencapsulated Wheat Germ Oil Attenuates Dose-dependent Titanium Dioxide Nanoparticles Hepatorenal Toxicity in Male Rats

Nagat D. Kotb

nagatdesouky@aast.edu

Arab Academy for Science, Technology and Maritime Transport

Mai M. Ali

Arab Academy for Science, Technology and Maritime Transport

Marium M. Shamaa

Arab Academy for Science, Technology and Maritime Transport

Mona AH. Yehia

Alexandria University

Sabah G. El-Banna

Studies Institute of Graduate Studies and Research Alexandria University

Article

Keywords: Titanium dioxide nanoparticles, wheat germ oil-nanostructured lipid carrier, oxidative stress, hepatotoxicity-nephrotoxicity, inflammatory cytokine (TNF-α), growth factor (GP88).

Posted Date: March 23rd, 2026

DOI: https://doi.org/10.21203/rs.3.rs-9102938/v1

License: This work is licensed under a Creative Commons Attribution 4.0 International License.
Read Full License

Additional Declarations: No competing interests reported.

Abstract

Titanium dioxide nanoparticles (TiO_2-NPs) are extensively used nanomaterials associated with oxidative stress mediated organ toxicity. This study investigated the dose-dependent hepatorenal toxicity of TiO_2-NPs in adult male rats and evaluated the protective efficacy of free and nanoencapsulated wheat germ oil (WGO), focusing on oxidative stress, inflammation, and DNA damage. WGO composition was characterized by gas chromatography–mass spectrometry (GC–MS), and its antioxidant activity was assessed *in vitro*. Hepatic and renal titanium accumulation analyzed using Inductively Coupled Plasma Emission Spectrometry ICP. Biomarkers of oxidative stress, liver and kidney function, antioxidant enzyme activities, and DNA damage were determined. Histopathological and immunohistochemical analyses were performed to assess tissue injury and inflammatory markers (TNF-α and GP88). WGO was rich in polyunsaturated fatty acids and demonstrated strong antioxidant activity. TiO_2-NPs exposure resulted in significant hepatic and renal titanium accumulation, elevated oxidative stress and DNA damage, impaired organ function, reduced antioxidant enzyme activities, and marked histopathological alterations with increased TNF-α and GP88 expression. Co-administration of WGO significantly attenuated these changes, with nanoencapsulated WGO providing greater protective effects than the free form of oil, likely through enhanced antioxidant and anti-inflammatory mechanisms, supporting its potential as a pharmacological strategy against nanoparticle-induced oxidative injury.

1. Introduction

The swift and extensive incorporation of metal oxide nanoparticles into industrial practices has led to a shift in the chronic human exposure profile, particularly with respect to titanium dioxide nanoparticles (TiO_2 NPs) **(Kotil et al., 2017)**, TiO_2 NPs have become the focus of major concerns owing to their extensive occurrence in food products (E171) and pharmaceuticals **(Sallam et al., 2022; Boutillier et al., 2022)**. Despite the varying regulations and guidelines related to the safety of TiO_2 NPs in different regions of the world, an increased amount of scientific evidence suggests the possibility of the bioaccumulative nature of TiO_2 NPs after accidental exposure routes **(Khan et al., 2025)**.). Once in the systemic circulation, the liver and kidneys act as the major physiological reservoirs of nanoparticles **(Zhang et al., 2024)** and become particularly susceptible to nanoparticle-induced injury **(Abdel-Halim et al., 2022)**.

The toxicological properties of titanium dioxide nanoparticles have primarily been related to the nitro-oxidative stress phenomenon. Enhanced surface reactivity of nanoparticles allows them to produce an increased amount of ROS/RNS, ultimately leading to the degradation of membrane phospholipids **(Manzoor et al., 2024; Dhupal et al., 2018)**. In the liver, this harmful effect of nanoparticles results in the disruption of metabolic processes and glucose and lipid metabolism **(Abuzaied et al., 2024)**. In the kidney cortex, the peroxidation of the glomerular membrane results in the accumulation of nitrogenous wastes and disruption of excretory processes **(Ghareeb, 2023)**.

In the face of ongoing global changes towards sustainable and environmentally friendly resources, research interest in bioactive natural products has been heightened. Due to the high lipophilicity of oils, there is a clinical need for innovative delivery systems. Bioactive matrix wheat germ oil (WGO) has been shown to possess antioxidant activity **(El-Bana et al., 2022)**, and thus has considerable hepatoprotective and renoprotective potential. can offer significant hepatoprotective and renoprotective potential. However, its therapeutic efficacy is often constrained by its poor oral bioavailability. This investigation evaluates a novel chitosan-coated nanostructured lipid carrier (NLC) system designed to augment the bioavailability **(Bashiri et al., 2020)** and intracellular delivery of WGO bioactive by providing a systemic antioxidant shield, this study aims to demonstrate a sustainable pharmacological strategy for maintaining hepatorenal integrity against the rising burden of nanoparticle-induced systemic toxicity.

2. Materials and methods

2.1 Materials

High-purity TiO_2 NPs (Quasi-spherical like shape, 50 ± 5nm), Fig. 1 were obtained from Nano Tech Egypt. Wheat germ oil was sourced from Imtenan Company Obour City, Egypt. Analytical-grade chemicals, including reduced glutathione (GSH), thiobarbituric acid reactive substances (TBARS), nicotinamide adenine dinucleotide phosphate (NADPH), cremophor RH-40 and chitosan, were procured from Sigma-Aldrich (USA). Clinical diagnostic kits for hepatorenal profiling were supplied by Biodiagnostic (Giza, Egypt) and Spectrum (Cairo, Egypt).

2.2 Methods

2.2.1 Gas chromatography-mass spectroscopy

The chemical constituents of the native WGO were characterized using Gas Chromatography-Mass Spectrometry (GC-MS) (Institute of Public Health, Alexandria University, Egypt). Separation was achieved on a capillary column using helium as the carrier gas, with bioactive compounds and fatty acid profiles identified via mass spectral matching against the NIST library database (test conditions are given in the supplemental file).

2.2.2 Total antioxidant capacity assay of wheat germ oil

Total antioxidant capacity of WGO was monitored according to **(Prieto et al., 1999)** (details of test conditions and calculations are summarized in the supplementary file).

2.2.3 Fabrication and physicochemical analysis of NLC loaded with wheat germ oil

WGO-loaded NLCs were synthesized via a melt-emulsification technique according to **(Souto et al., 2019)** with some modifications followed by high-speed homogenization method using High-shear homogenizer

(Unidrive CAT1000 CAT Scientific) (10,000 rpm) and ultra-sonication (probe sonicator; Vibra-Cell). The resulting NLCs was surface-modified with a 0.5% chitosan coating to optimize gastrointestinal retention **(Hassan et al., 2024).** The comprehensive compositional data for the investigated formulations are presented in Table 1. The colloidal properties, including particle size and polydispersity index (PDI), were determined through dynamic light scattering (DLS) using (Malvern Zeta Sizer Nano-ZS; UK). Morphological characterization was performed via Transmission Electron Microscopy (TEM, Jeol JEM-1400 Plus, USA) to visualize particle shape and uniformity **(Shi et al., 2012)**. To assess the loading capacity, entrapment efficiency (EE%) was determined using an indirect ultrafiltration methodology **(Li et al., 2009)**, with unentrapped oil quantified via UV-Visible spectrophotometry (Pg model T80+).(details of each test are summarized in the supplementary file).

Table 1
Formulation and optimization of nanostructured lipid carrier loaded with wheat germ oil

Formulation code	Homogenization (min)	Ultra sonication (min)	w/w % Oily phase : aqueous : SPAN			Water
			Cetyl alcohol: WGO (1:2)	**Cremophor RH40**	**SPAN 80**	
F1	**10**	**-**	**3**	**3**	**1**	**To 10g**
F2	**10**	**-**	**6**	**3**	**1**	
F3	**15**	**-**	**3**	**3**	**1**	
F4	**20**	**-**	**3**	**3**	**1**	
F5	**10**	**5**	**3**	**3**	**1**	
F6*	**10**	**5**	**3**	**3**	**1**	**To 8g**
F7* placebo	**10**	**5**	**3**	**3**	**1**	

*** F6, F7 weight was completed to 10 g using chitosan solution**

2.2.4 Animal study

Sixty adult male Wistar rats (146 ± 5 g), sourced from animal house, Faculty of Medicine, Alexandria University. Animals were randomly assigned to ten experimental cohorts (n = 6) and acclimated under standardized conditions (22 ± 2°C) with a 12:12-h light/dark photoperiod. TiO_2 NPs were dispersed in saline via ultra-sonication (Ultrasonic bath sonicator Branson_CPX2800) for 15 min to assure no significant agglomeration in the aqueous dispersion took place, and administered intraperitoneally (200 µL) at 5 mg/kg (Tid1) and 25 mg/kg (Tid2) **(Abdel-Halimet al., 2022; Salmanet al., 2021; Youneset al., 2015)**. Prophylactic WGO (free or NLC-encapsulated) was administered via oral gavage at a dose of 270 mg/kg **(Husseinet al., 2014).** Dosing commenced three days per week for six weeks, with administrations occurring at approximately the same time, as detailed in Table 2. The study was

approved by the Institutional Animal Care and Use Committee **(AU14-230614-2-4)** and adhered to all guidelines for experimental animal use **(Festing and Altman, 2002)**.

Table 2
Experimental animal design

Group	Treatment
Group I	**control intraperitoneal administered with saline**
Group II	**administered with (270 mg/kg B.W) of WGO**
Group III	**administered with (270 mg/kg B.W) of WGO NLC**
Group IV	**administered with blank NLC (placebo)**
Group V	**administered with (5 mg/kg B.W) of TiO_2 NPs (Tid1)**
Group VI	**administered with Tid1 + WGO**
Group VII	**administered with Tid1 + WGO NLC**
Group VIII	**administered with (25 mg/kg B.W) of TiO_2 NPs (Tid2)**
Group IX	**administered with Tid2 + WGO**
Group X	**administered with Tid2 + WGO NLC**

2.2.4.1 Hepatorenal biochemical profiling (Serum)

Following the six-week period, rats were anesthetized via isoflurane inhalation, and blood was harvested via cardiac puncture in clot activator tubes. Serum was separated for the quantification of hepatic integrity markers (GGT, ALP, BChE, ALT, AST) **(Persijn and van der Slik, 1976; Belfield and Goldberg, 1971; Knedel and Böttger, 1967; Reitman and Frankel, 1957)**, albumin **(Doumas et al., 1971)**, bilirubin **(Price et al., 1976)**, glucose **(Weissman and Klein, 1958)**, renal filtration indices (urea, uric acid and creatinine) **(Patton and Crouch, 1977; Barham and Trinder, 1972; Schirmeister, 1964)**, lipid profile **(Assmann et al., 1984; Richmond, 1973; Bucolo and David, 1973)**. All assays were performed according to standard clinical methodologies.

2.2.4.2 Metabolic and oxidative status in tissue homogenates

Liver and kidney tissue homogenates were prepared **(Kaplan and Utiger, 1978)** with some modification briefly, a selected weight of tissue was homogenized in 0.1mol/L phosphate buffer saline, pH 7.4 (1:4 w/v for liver) and (1:5 w/v for kidney), using a Teflon-glass homogenizer (WiseTis Homogenizer HG 15D) at 4 ºC. The total homogenate was centrifuged (11,000 rpm) under cooling (4 ºC) for 20 min. Supernatant stored at -80 ºC for subsequent biochemical studies. Metabolic status was evaluated by quantifying Total lipids, total hepatic content of aniline 4-hydroxylase, amidopyrine N-demethylase,

CYP_{450} and cytochrome b_5, NADPH- cytochrome c reductase, activities were determined as described by **(Frings et al., 1972; Kato and Gillette, 1965; Omura and Sato, 1964; Williams Jr and Kamin, 1962; Nash, 1953)** respectively. The peroxidative burden was assessed through malondialdehyde **(Tappel and Zalkin, 1959)** and nitric oxide concentrations **(Montgomery, 1971)**. The endogenous antioxidant status was determined by measuring GR, GST, SOD, CAT and GPx activities **(DM, 1983; Habig et al., 1974; Nishikimi et al., 1972; Sinha, 1972; Paglia and Valentine, 1967)** respectively alongside reduced GSH levels **(Ellman, 1959)**. DNA fragmentation was quantified using the diphenylamine reaction to assess chromosomal stability **(Wu et al., 2006)** (details are summarized in the supplementary file).

2.2.4.3 Determination of Titanium content in tissues

For the determination of titanium tissue bioaccumulation, samples underwent microwave-assisted acid digestion (nitric acid/H_2O_2) and were analyzed using Inductively Coupled Plasma Emission Spectrometry (ICP-ES Agilent 5100 VDV) according to **(Eilola and Perämäki, 2001)** with some modification (details of each test are summarized in the supplementary file).

2.2.4.4 Histological and immunohistochemical evaluation

Liver and kidney tissue histology specimens were examined according to **(Suvarna et al., 2018)**. Immunohistochemical (IHC) mapping of TNF-α and GP88 was performed according to **(Salguero et al., 2001)** (details are summarized in the supplementary file).

2.2.5 Statistical analysis

Quantitative data are presented as mean ± standard error. Group comparisons were performed using one-way ANOVA followed by Tukey's HSD (SPSS v.14.0). Statistical significance was defined as $p < 0.05$ (**(Norušis, 2006).**

3. Results and discussion

3.1 Gas chromatographic - mass spectroscopic analysis of wheat-germ oil

The GC-MS analysis of WGO successfully identified 22 distinct compounds by comparing their mass spectra with established spectral libraries. Of these, the most significant compounds, constituting approximately 90% of the total WGO composition, are detailed in Table 3. The analysis confirms that WGO is predominantly composed of unsaturated fatty acids, with linoleic acid being the most abundant, followed by palmitic and oleic acids. This finding agrees with multiple independent studies **(Zargar et al., 2023; Emam et al., 2022)**.

Table 3
Gas chromatographic - mass spectroscopic analysis of wheat germ oil

Compound Name	Molecular Formula	RT	Area %
9,12 Octadecadienoic acid (Z,Z) (Linoleic acid) (omega-6)	$C_{18}H_{32}O_2$	32.83	65.07
n Hexadecanoic acid (Palmitic acid)	$C_{16}H_{32}O_2$	29.72	16.45
Oleic acid (omega-9)	$C_{18}H_{34}O_2$	33.02	5.73
9,12 Octadecadienoyl Chloride (Z,Z) (Linoleoyl chloride)	$C_{18}H_{31}C_{lO}$	37.21	2.85
9Hexadecenoic acid (palmitoleic acid) (omega 7)	$C_{16}H_{30}O_2$	35.60	2.00
9,12,15-octadecatrienoic acid (linolenic acid) (omega-3)	$C_{18}H_{30}O_2$	37.35	0.48
3,7,11,15-tetramethylhexadec-2-en-1-ol (phytol, acetate)	$C_{22}H_{40}O_2$	27.05	0.42

The identified components of WGO possess various bioactivities. Linoleic acid is an essential omega-6 PUFA that is associated with decreased cardiovascular morbidity **(Sacks et al., 2017)**, displays antioxidant activity, anti-mutagenic and anti-tumorigenic effects **(Dachev et al., 2021).** Palmitic acid exhibits anti-inflammatory, metabolic regulatory, hypocholesterolemic, anticancer and antiproliferative effects **(Zhu et al., 2021)**. Oleic acid demonstrates potential in cancer prevention, particularly breast cancer, and contributes to improved lipid profiles by increasing HDL, decreasing LDL cholesterol. Furthermore, it has been shown to reduce insulin resistance, enhance energy and cognitive function, and modulate the immune system **(Wang et al., 2025)**. Another several fatty acids and their derivatives like Alpha-linolenic acid, an omega-3 PUFA, helps reduce cardiovascular disease risk by improving lipid profiles **(Naghshi et al., 2021)**, Similarly, linoleoyl chloride offers diverse benefits such as being anticoronary, hypocholesterolemic, and hepatoprotective **(Vijayabaskar and Elango, 2018)**, Palmitoleic acid, an omega-7 fatty acid, enhances insulin sensitivity, potentially lowering diabetes risk **(Hu et al., 2019b)**, finally, phytol derivatives like phytol acetate provide antioxidant, anticancer and anti-inflammatory properties, protecting against oxidative stress and the development of cancer **(Shalabi and Eskander, 2022)**.

3.2 Determination of total antioxidant capacity (TAC) of wheat germ oil

Due to the significant influence of reactive oxygen species (ROS) in the oxidative damage of vital biomolecules, quantifying the Total Antioxidant Capacity (TAC) of protective phytoconstituents derived from natural sources, such as wheat germ oil, became a primary focus of research. **(Ghagane et al., 2017).** In this work, TAC of WGO was estimated by phosphomolybdenum method **(Zaveri, 2021).** The obtained results (expressed as vitamin E equivalent) presented in Fig. 2 revealed that the reducing ability of WGO increased with the increase in the oil concentration and that WGO has a high TAC in comparison to the established lipophilic antioxidant reference vitamin E the results agree with **(Wu et al., 2022)**.

3.3 Preparation and Physicochemical characterization of WGO NLCs

3.3.1 Preparation of WGO NLCs

Wheat germ oil encapsulation in a lipid-based nano-delivery system particularly nanostructured lipid carriers (NLCs) was selected due to their generally reported superior activity to free oil in terms of delivery and bioavailability **(Bashiri et al., 2020)**. NLCs were selected rather than nanoemulsion for the reported higher physical stability and protection of the valuable polyunsaturated components of WGO. Cetyl alcohol was selected for its comparatively low melting point (49.3°C) as the solid lipid to avoid long exposure to high temperature during NLCs preparation that may negatively affect the oil components **(Apostolou et al., 2021)**.

Nanoparticle colloidal properties dictate stability and influences biological interactions including pharmacokinetics and cellular uptake, primarily affecting the initial binding to the cell membrane, **(Honary and Zahir, 2013)**, and phagocytosis **(Guo et al., 2018; Remya and Damodharan, 2018).** Colloidal characteristics of the prepared NLCs formulations are shown in Table 4.

Table 4
Characterization of nanostructured lipid carrier loaded with wheat germ oil

Formulation code	Oily phase: aqueous phase: SPAN % w/w	Condition (min)		Colloidal properties		
		Homogenization	Ultra sonication	Size	PDI	Zeta potential
F1	3:3:1	10	-	192.0 ± 0.23	0.453 ± 0.0	-23.5 ± 0.29
F2	6:3:1	10	-	364.1 ± 0.64	0.710 ± 0.01	-16.9 ± 0.23
F3	3:3:1	15	-	186.8 ± 1.73	0.539 ± 0.01	-21.2 ± 0.23
F4	3:3:1	20	-	265.9 ± 1.96	0.600 ± 0.03	-46.2 ± 0.40
F5	3:3:1	10	5	189.0 ± 0.29	0.334 ± 0.01	-55.0 ± 0.29
F6*	3:3:1	10	5	173.9 ± 0.51	0.39 ± 0.01	14.4 ± 0.23
F7* placebo	3:3:1	10	5	185.9 ± 0.40	0.395 ± 0.0	12.7 ± 0.35
The results are expressed as (Mean ± SE,n = 3)						

3.3.1.1 Effect of %w/w oily phase

Results in Table 4 showed that formulation (F2) containing 6% w/w lipids exhibited significantly higher particle size and PDI than formulation (F3) containing 3% w/w lipids. This may be attributed to the higher viscosity of the 6% w/w lipids which prevents oil droplets breakdown during preparation in accordance with previously reported data **(Gilani et al., 2022).** In addition, a reverse relation was observed between w/w % of lipids and colloidal stability where zeta potential increases with the decrease in w/w lipids. To improve the colloidal characteristics of the selected smaller, more homogenous and stable formulation (F1), size reduction method including increasing homogenization time and ultrasonication were studied

3.3.1.2 Effect of size reduction method

In formulations (F1 and F3), it was noticed that, increasing homogenization time from 10 to 15 min. resulted in a slight non-significant ($P < 0.05$) decrease in particle size accompanied by a similar decrease in the homogeneity and stability as seen from the results. However, extending the homogenization time to 20 min. (F4) resulted in total loss of homogeneity and stability where a significant size increase is noticed due to the coalescence of small droplets into stable larger droplets. These results are consistent with previously reported data **(Gilani et al., 2022; Ajiboye et al., 2021).** In formulations (F1 and F5), five minutes ultrasonication resulted in a non-significant particle size decrease, however, a significant improvement ($P > 0.05$) in colloidal homogeneity and stability of the prepared formulation was seen. From the above results, a formulation (F5) showing suitable colloidal characteristic was selected for further studying.

3.3.1.3 Effect of chitosan coating

For enhancing the oral delivery (absorption and bioavailability) of the prepared NLCs, the formulation (F5) was surface-coated with the mucoadhesive polymer, chitosan, **(Aibani et al., 2021).** As seen from Table 4, chitosan coating resulted in a slight decrease in particle size and homogeneity compared to the uncoated NLCs. Critically, the zeta potential shifted from **(-55 mV**) to **(+ 14.4 mV**), confirming successful surface coating with the cationic polymer chitosan. This positive surface charge can possibly enhance NLCs adhesion to the negatively charged cell membranes in the GIT, potentially enhancing in-vivo absorption and cellular accumulation of the prepared NLCs **(El-Nashar et al., 2022).**

3.3.2 EE %

The obtained results indicate a high EE % (99.65% ± 0.05) in the selected formulation (F6). This notably high encapsulation efficiency is likely attributable to the substantial solubility of WGO within the lipid matrix, coupled with its inherent hydrophobic nature, which collectively minimized its partitioning into the external aqueous phase.

3.3.3 Morphological analysis using transmission electron microscope (TEM)

The optimized WGO-loaded NLC formulation (F6) showed nanoparticles with a smooth surface and a homogeneous spherical shape with a well-defined morphology and a particle size range of approximately 45 to 65 nm, as represented by Fig. 3.

3.4 Animal Study

To evaluate the oxidative stress-induced toxicities of TiO_2 nanoparticles (NPs) in animal models, a comprehensive approach is necessary, where not only the circulating biomarkers in the blood are considered, but also the target organs, such as the liver and kidneys, are examined directly. This methodological approach also allows for the evaluation of the effectiveness of the antioxidant preventive measures, which in the current study are implemented in the form of the co-administration of free or nano-encapsulated wheat germ oil and TiO_2 NPs.

3.4.1 Biochemical analysis of blood serum of male rats.

The functional integrity of the liver and kidneys, (primary organs for metabolism and excretion), is reliably reflected by numerous systemic circulating biomarkers. These markers offer crucial insights into cellular damage, metabolic shifts, and inflammatory processes within these organs. Evaluating these systemic biomarkers following exposure to TiO_2 NPs doses, can delineate the extent of induced hepatorenal dysfunction, while evaluation after concurrent administration of free or nanoencapsulated WGO can outline their protective effects **(Tamber et al., 2023; Lash, 2022)**.

3.4.1.1 Fasting blood sugar (FBS)

The intraperitoneal injection of TiO_2 NPs to male rats caused dose-dependent hyperglycemia by increasing fasting blood glucose levels compared to the control groups Fig. 4a. The effect of TiO_2 NPs on blood glucose levels is consistent with previous studies that showed that exposure to TiO_2 NPs could affect blood glucose levels **(Hu et al., 2018; Vasantharaja et al., 2015)**. The liver plays the main role in the regulation of blood glucose homeostasis, and it achieves this through precise cellular mechanisms in the processes of glycogenesis. All these processes are controlled in a precise manner. In the hepatocyte, the endoplasmic reticulum and cytochrome P450 enzymes are the two main regulators of the metabolic process **(Hu et al., 2019a)**. The exposure of cells to TiO_2 NPs could decrease the level of cytochrome P450 enzymes and cause endoplasmic reticular stress in the liver cells of rats exposed to TiO_2 NPs. The effect of TiO_2 NPs could potentially activate a local inflammatory response in liver cells that could affect the organism's response to blood glucose levels by causing insulin resistance **(Shin et al., 2019; Hu et al., 2019a)**. The effect of TiO_2 NPs on blood glucose levels has demonstrated that metal-based NPs could affect blood glucose levels and potentially cause metabolic diseases similar to type 2 diabetes *mellitus* **(Priyam et al., 2018; Heller et al., 2018)**.

Interestingly, concurrent administration of WGO significantly prevented the TiO_2 NPS induced glucose dysregulation. This protective effect is primarily attributed to WGO's inherent rich composition of

bioactive antioxidant constituents, known to positively influence insulin signaling and glucose metabolism **(Hamilton and Klett, 2021)**. The observed amelioration of hyperglycemia by WGO in this study aligns with previous reports demonstrating its efficacy in mitigating glucose dysregulation in diet-induced metabolic disorders **(Nagib, 2018; Orabi et al., 2016)** Notably, the protective efficacy of WGO was observed to be superior in its free form compared to encapsulated formulations, suggesting that the delivery and bioavailability of its active compounds are critical for its preventative bioactivity additionally, free essential oils are lipophilic, so they cross cell membranes easily on their own can directly interact with intestinal enzymes (α-amylase, α-glucosidase) and improving insulin sensitivity at the membrane **(de Sousa et al., 2024)** while, nanoformulations may bypass early gut interaction.

Lipids profile

TiO_2 NPs administration to male rats induced a significant and dose-dependent increase in serum TC, TG, and LDL-c, accompanied by a dose-dependent decrease in HDL-c, compared to the control group Fig. 4b. These results are consistent with previous findings, where TiO_2 NP exposure has been shown to induce dyslipidemia in animal models **(Boughediri et al., 2024)**. From a mechanistic perspective, TiO_2 NPs are thought to affect lipid homeostasis in hepatocytes by causing oxidative stress, which in turn may affect important enzymatic activities and/or signaling pathways involved in lipid synthesis and metabolism. Moreover, TiO_2 NPs may also affect the activity of lipoprotein lipase, thereby influencing lipid kinetics.**(Salman et al., 2021)**.

On the other hand, the concurrent administration of WGO in both its free and nano-encapsulated forms was generally associated with the maintenance of lipid homeostasis in both concentrations of TiO_2 nanoparticles by reducing the increase in total cholesterol (TC), triglycerides (TG), and low-density lipoprotein cholesterol (LDL-c) in the serum. These results suggest that WGO shows a partial protective effect (not significant different from the negative control group). These results are in agreement with the results of previous studies **(Naghshi et al., 2021; Saleh, 2016a)** which showed that the oral administration of free WGO significantly improves lipid profiles in rats with diet-induced hyperlipidemia and protects against liver damage caused by carbon tetrachloride (CCl_4).

Moreover, it was noted that free WGO was more effective than nano-encapsulated WGO for most of the lipid profiles, except for HDL-c, which showed significantly better protective activity of nano-encapsulated WGO compared to free WGO in both concentrations of TiO_2 NP-treated groups. This may be due to the fact that nano-encapsulation is a method that optimizes the bioavailability of the components of free WGO to the sites of action **(Naghshi et al., 2021; Sacks et al., 2017)** pertinent to the synthesis of HDL-c in the cell. Thus, it is expected that the components of free WGO may be present in lower concentrations within the cell compared to the nano-encapsulated lipid core (NLC) formulation of WGO, which may be present in greater concentrations within the cell to produce a greater preservation of HDL-c levels compared to free WGO.

Serum protein and bilirubin profile

The role of the liver in synthesis and excretion is a key factor in maintaining systemic homeostasis, with a variety of circulating proteins and bilirubin acting as the main biomarkers. The total protein (TP) and albumin indices are related to the synthetic ability of the liver, and a decreased albumin/globulin (A/G) index, a sensitive marker for a variety of diseases, including inflammation, cirrhosis, autoimmune diseases, and certain neoplastic conditions **(Philips et al., 2020)**. Bilirubin, a by-product of heme degradation, is conjugated by hepatocytes and then excreted into the bile. An increase in indirect (unconjugated) bilirubin is a sign of impaired uptake and conjugation, and an increase in direct (conjugated) bilirubin is a sign of impaired excretion.

With respect to the current investigation, the hepatotoxicity of TiO_2 NPs was evident in rats as a function of dose, as demonstrated in Fig. 4c. The substantial increases in TP and bilirubin levels, along with decreased albumin levels and the albumin-globulin ratio indicate a high level of hepatotoxicity. Furthermore, the increases in indirect and direct bilirubin levels indicate a failure of hepatocellular conjugation and excretion of the latter via the biliary system. The results are in accordance with previous studies indicating that exposure to TiO_2 NPs causes hepatotoxicity by disrupting liver function to elevate bilirubin and TP levels and decrease albumin levels **(Boughediri et al., 2024; Salman et al., 2021; Chen et al., 2019)**. The mechanism of hepatotoxicity caused by TiO_2 NPs involves oxidative stress, which may directly damage hepatocytes and disrupt the activity of the critical enzyme uridine-diphosphoglucuronic glucuronosyltransferase (UDPGT) for the conjugation of bilirubin to a water-soluble derivative for excretion into the bloodstream. The disruption of this enzyme activity causes the accumulation of indirect and direct bilirubin levels. In addition to oxidative stress, exposure to TiO_2 NPs may also cause damage to and obstruction of bile ducts, specifically for the excretion of direct bilirubin **(Tripathi and Jialal, 2020)**. The clinical significance of the hepatotoxicity of TiO_2 NPs is substantial because the substantial alterations of liver function test parameters indicate a high level of hepatotoxicity that may cause substantial cardiovascular and neurological comorbidities.

On the other hand, co-administration of WGO significantly reduced hepatotoxicity caused by TiO_2 NPs, and nanoencapsulated WGO exhibited more potent activity than its free form. Although the free form of WGO partially corrected serum levels, nanoencapsulated WGO completely prevented changes in total protein and albumin levels, thus maintaining hepatic synthetic function. Furthermore, nanoencapsulated WGO exhibited significantly higher potential than its free form in maintaining bilirubin levels, reflecting the greater potential of nanoencapsulation to protect hepatocellular integrity and biliary function. The hepatoprotective activity of nanoencapsulated WGO could be attributed to its potent antioxidant properties, which proactively counteract oxidative stress and inflammation caused by TiO_2 NPs, thus maintaining hepatocellular integrity and function. The results of this study are consistent with earlier studies showing that WGO has potent potential to protect against various xenobiotic-induced liver toxicities, such as chlorpyrifos **(Khalifa et al., 2011)**, nicotine **(Abdallah and Bakry, 2014a)**, and doxorubicin **(Soliman et al., 2015)**. The more potent activity of nanoencapsulated WGO could be attributed to the potential advantages offered by nanoencapsulation technology, such as enhancing the bioavailability and targeted delivery of its active constituents.

Liver function

The structural and functional integrity of the liver is vital to accomplish these roles. Hepatocyte injury or cholestasis can be diagnosed through changes in circulating hepatic enzymes, which are sensitive indicators of liver health. For instance, increased concentrations of circulating ALT, AST, ALP, GGT, and BChE are often indicative of liver injury/dysfunction, which may be related to changes in hepatocyte membrane permeability and/or impaired biliary excretion **(Sherif et al., 2019)**. Additionally, alanine transaminase and aspartate transaminase are generally sequestered in the cell and localized in the cytosol for ALT and in the cytosol and mitochondria for AST. So, AST/ALT ratio has been demonstrated to be effective in identifying cirrhosis across diverse liver disorders **(Yang et al., 2018)**.

The current investigation found that treatment with TiO_2 nanoparticles induced a statistically significant dose-related increase in circulating AST, ALT, ALP, BChE, and GGT with a significant reduction in AST/ALT ratio in male rats compared to the control group Fig. 4d,e. This increase in circulating liver enzymes suggests compromised integrity of the hepatocyte membrane, resulting in the leakage of intracellular enzymes into the bloodstream, which is characteristic of liver injury **(Chang et al., 2023)**. A lower ratio of AST to ALT release observed in the TiO_2 NPs treated group (at both doses) is often noted in the early to moderate stages of liver injury. This is because ALT, being a cytosolic enzyme, tends to leak out of the cell more easily upon disruption of the cell membrane. In contrast, AST leakage from mitochondria tends to require a greater amount of cellular injury **(Contreras-Zentella and Hernández-Muñoz, 2016)**. These decreases in the AST/ALT ratio indicate oxidative stress-induced and loss of membrane integrity of the hepatocytes as previously reported by **(Guo et al., 2009)**.

The TiO_2 nanoparticles may be capable of producing ROS, which may lead to oxidative stress in hepatocytes, potentially triggering lipid peroxidation, which may compromise the integrity of the plasma membrane. These findings are in agreement with emerging scientific evidence showing increased concentrations of circulating liver enzymes following oral and ip administration of TiO_2 nanoparticles to laboratory animals **(Vasantharaja et al., 2019; Hassanein and El-Amir, 2017; Fatemeh and Mohammad, 2014)**.

Beyond hepatocellular integrity, the observed increase in serum ALP aligns with the rise in indirect and direct bilirubin which suggested failed biliary excretion, indicating potential cholestatic injury, which can also damage hepatocyte membranes **(Levitt et al., 2022)**. Furthermore, elevated ALP may indicate chronic kidney disease **(Zhu et al., 2016)**, thus necessitating a broader assessment of its function given ALP non-specificity. Similarly, the concurrent elevation of BChE, while primarily a marker of liver function, it may also indicate central nervous system (CNS) problems that aligns with the observed glucose dysregulation and its known detrimental effects on CNS integrity **(Strand et al., 2024)**.

The co-administration of wheat germ oil, in both free and nano-encapsulated forms, was seen to significantly mitigate the manifestations of hepatotoxicity caused by TiO_2 nanoparticles. This is explained by the high levels of antioxidants and bioactive compounds present in wheat germ oil, which

work synergistically to reduce the oxidative stress caused by these particles. This conclusion is supported by previous studies showing the hepatoprotective effects of WGO against various toxic insults, such as thioacetamide-induced hepatotoxicity **(Alamery et al., 2022)** and elevated levels of liver enzymes caused by methotrexate **(Saleh, 2016b)**.

Kidney functions

Nephrotoxicity leads to impaired kidney function in the removal of waste products from the body and electrolyte balance. Serum levels of urea and creatinine are used to monitor impaired kidney function by reduced levels of glomerular filtration rate; variations in uric acid levels are associated with a complex interplay between excretion by the kidney **(Park et al., 2020)** and hepatic metabolism **(Alidadi et al., 2018)**. In the present study, administration of TiO_2 NPs to male rats caused a significant increase in serum levels of creatinine and urea Fig. 4a, and a significant decrease in serum uric acid levels was observed Fig. 4e indicating impaired kidney function in terms of reduced glomerular filtration rate or renal excretory capacity compared to the control group. TiO_2 NPs may cause oxidative stress in the kidney by the formation of ROS, which may cause inflammation and damage to the kidney, ultimately affecting the renal tubules and glomeruli. On the other hand, a significant reduction in serum levels of uric acid was observed Fig. 4e. This may be due to reduced levels of uric acid formation or reduced reabsorption from the renal tubules **(Park et al., 2020)** which indicates underlying kidney pathology with considerable clinical implications. This study strongly supports previous studies where significant increases in levels of blood urea and creatinine and decreases in levels of uric acid were observed after exposure to TiO_2 NPs in animal models **(Ghareeb, 2023; Wani et al., 2021; Morgan et al., 2017b)**.

Conversely, the efficacy of the combination of WGO and WGO-loaded in nanoencapsulated form WGO NLC in the prevention of the nephrotoxic effects of TiO_2 NPs, as evidenced by the normalization of serum urea, creatinine, and uric acid levels, is plausible and can be attributed to the nephroprotective efficacy of the bioactive compounds in WGO, which counteract the oxidative stress and inflammation caused by the exposure to TiO_2 NPs, thereby preserving the integrity of the structure and function of the kidneys. This is in agreement with previous studies on the nephroprotective efficacy of WGO against a wide array of nephrotoxins, as demonstrated by its ability to counteract the nephrotoxic effects of gentamicin **(Hafez et al., 2019)** and cisplatin **(El-Bana et al., 2022)**. Again, the enhanced efficacy of WGO NLC over the free form is demonstrated in the current study.

Biochemical analysis in tissue homogenates of male rats.

To complement results of systemic biomarker assessments of TiO_2 NPS induced hepatic and nephrotoxicity, biochemical analyses were performed on liver and kidney homogenates. These analyses allow for quantification of damage in the target organs, providing localized insights into the cellular responses to TiO_2 NPs exposure and protection by WGO beyond circulating indicators.

3.4.1.5 Titanium accumulation study

The results of Titanium (Ti) accumulation using ICP-MS, confirmed significant Ti accumulation in liver and kidney tissues following TiO_2 NPs exposure in Tid2 group (26.4 µg/g in liver and 15.56 µg/g in kidney tissues). These findings support reported data that TiO_2 NPs can circulate systemically, and accumulate within vital organs **(Wani et al., 2021; Heringa et al., 2018)**. Remarkably, concurrent administration of WGO in the free and nano-encapsulated forms completely prevented detectable Ti accumulation in these organs. This result may be explained by the antioxidant and anti-inflammatory properties of WGO, which probably protected liver and kidney histological and physiological integrity to an extent that the body was able to prevent the absorption of the injected TiO_2 (forming a barrier) and prevent its accumulation. This hypothesis may be supported by the above serum results related to liver and kidney functions where WGO in its free and nanoencapsulated forms was able to significantly improve the studied indices and can offer an effective approach to mitigate Ti accumulation and associated TiO_2 NPs induced organ toxicity.

Liver total lipids and cholesterol

The obtained results expressed in Fig. 5a,b show that, exposure to TiO_2 NPs significantly elevated total lipids and cholesterol in liver homogenate in a dose dependent manner in agreement with **(ANI et al., 2008)** and indicating a dose dependent impairment of lipid metabolism in the liver.

Interestingly, in the low dose TiO_2 NPs group, concurrent administration of free or nanoencapsulated WGO significantly prevent these elevations and the results were not significantly different from control group. However, in the high dose TiO_2 NPs group WGO although significantly attenuated these elevations, but results were still significantly higher than control group. These findings suggest that WGO (both in its free and nano-encapsulated forms), through its antioxidant and anti-inflammatory properties, exerts a protective effect against TiO_2 NPs induced impairment of lipid metabolism in the liver, agreeing with previously reported data **(Ismael et al., 2014)**.

Notably, while WGO-NLC more effectively controlled total lipids, free WGO exhibited a superior capacity to maintain cholesterol homeostasis. The increased efficacy of free WGO can be accounted for based on the ability to enhance the biotransformation of cholesterol into bile acids, in addition to disrupting the enterohepatic circulation of cholesterol through the inhibition of reabsorption and the enhancement of excretion. On the other hand, the enhanced efficacy of nanoencapsulated WGO in the reduction of total lipid levels can be accounted for based on the ability to enhance intracellular delivery to organelles such as the endoplasmic reticulum and mitochondria, thereby modulating lipid synthesis and catabolism. This indicates that the system of delivery plays a critical role in the modulation of the targeted metabolic pathway, with the overall lipid metabolism pathways being the focus of nanostructured lipid carriers NLC, rather than the bile acid synthesis pathways targeted by free WGO.

Liver metabolic enzymes

These findings, as shown in Fig. 5 **(a, c, d)** indicate that there were significant decreases in aniline 4-hydroxylase activity. These decreases indicate that TiO_2 NPs directly disrupt the enzyme's heme group

and compromise its ability to metabolize aromatic compounds **(Fröhlich et al., 2010)**. Additionally, the inhibitions of NADPH-cytochrome c-reductase and cytochrome b5 activities, as seen in our study and in **(Taş et al., 2020)**, suggest that there is a disruption of the electron transport mechanism that is critical in CYP metabolism. These decreases in enzyme activities can be attributed to TiO_2 NP-induced oxidative stress that fundamentally disrupts the integrity of these enzymes and ultimately causes widespread damage to the hepatocytes.

On the other hand, total Cytochrome P450 content and aminopyrine N-demethylase activities were found to be upregulated in response to lower concentrations of TiO_2 NPs. These two enzyme activities were found to be upregulated concurrently. These findings suggest that there is an adaptive response to counteract nanoparticle-induced oxidative stress. However, in response to higher concentrations of TiO_2 NPs, total P450 content was significantly decreased. These findings suggest that there is extensive damage to the metabolic machinery of the liver. The extensive damage is consistent with previous studies **(Fadda et al., 2018)**. Aminopyridine N-demethylase activity, however, was significantly upregulated at higher TiO_2 NP concentrations. These findings suggest that there is prioritization of detoxification pathways to counteract overwhelming toxicity.

The co-administration of free and nano-encapsulated WGO significantly reduced hepatotoxicity of TiO_2 NPs, as observed previously with **(Liu et al., 2022)**. This is evident through the retention of total Cytochrome P450 (CYP) content at near-physiological levels with all concentrations of TiO_2 NPs, as well as prevention of depletion of aniline 4-hydroxylase, NADPH-cytochrome c-reductase, and cytochrome b5. At the same time, it inhibited compensatory overexpression of aminopyrine N-demethylase activity observed with TiO_2 NP-only treated groups. Notably, this protective activity was dose-dependent, as with lower concentrations of TiO_2 NPs, free and nano-encapsulated WGO exhibited similar efficacy, while with high concentrations of TiO_2 NPs, where oxidative stress was high, there was clear superiority of the latter over free WGO, as it more effectively prevented total CYP content loss and overall enzymatic dysfunction.

The relative efficacy of free and nano-encapsulated WGO can be explained through differences in delivery kinetics to the endoplasmic reticulum, where all of these enzymes are located. As a lipophilic oil, free WGO would presumably be taken up rapidly through direct diffusion into hepatocytes, although this would be limited through rapid metabolism and clearance, thus constraining its protective window of action. Nano-encapsulation of WGO would presumably enhance bioavailability, as well as uptake through endocytosis, thus providing a more sustained delivery of bioactive components, providing a constant antioxidant effect that would be particularly important with aminopyrine N-demethylase activity, as it would counteract severe oxidative stress induced by TiO_2 NPs. While free WGO would presumably provide an instantaneous delivery of antioxidants, this would not provide as all-encompassing an effect as would be provided through nano-encapsulation, where a sustained delivery would be achieved through endocytosis, thus providing a more effective protection against TiO_2 NP-induced toxicity.

Oxidative stress

Thiobarbituric acid reactive substances (TBARS)

Oxidative stress is a key component of the mechanism of toxicity induced by TiO_2 NP exposure. Overproduction of ROS by TiO_2 NPs initiates a chain reaction that mainly attacks polyunsaturated fatty acids of the cell membranes, resulting in lipid peroxidation (LPO) and compromising the integrity of the membranes. Malondialdehyde (MDA) is one of the most significant end-products of lipid peroxidation that can be quantitatively measured by the thiobarbituric acid-reactive substances (TBARS) test and is well established as a reliable biomarker of oxidative stress-induced damage to the membranes. Moreover, overproduction of ROS by TiO_2 NPs may also be involved in the process of fibrogenesis by interacting with biomacromolecules and increasing the levels of fibrogenic growth factors and tumor necrosis factor-alpha (TNF-α), thus playing a significant role in the progression of liver diseases such as hepatitis C and fatty liver disease **(Akool, 2019)**. As depicted in Fig. 6a, TiO_2 NP exposure significantly increases lipid peroxidation because of the dose-dependent elevation of MDA levels in the liver and kidneys compared with controls. The increased levels of MDA suggest significant oxidative stress and lipid peroxidation reactions caused by TiO_2 NP exposure. This is consistent with previous reports of TiO_2 NP-induced oxidative stress and lipid peroxidation **(Abuzaied et al., 2024; Abdou et al., 2019; Shakeel et al., 2016; Orazizadeh et al., 2014).** Moreover, the increased levels of lipid peroxidation in the liver compared with the kidneys are also consistent with expectations because of the higher polyunsaturated fatty acid content of liver tissue and the liver's role as the primary site of lipid metabolism. This systemic toxicity may be compounded by oxidative damage to the kidneys, where lipid peroxidation of the renal interstitial tissue can inhibit erythropoietin synthesis and thereby limit the bone marrow's ability to compensate for anemia.

Remarkably, the simultaneous oral co-administration of free and nanoencapsulated WGO significantly attenuated LPO caused by TiO_2 NPs in liver and kidney tissues Fig. 6a. The effects of the low-dose TiO_2 NPs exposure were completely inhibited, while the high-dose TiO_2 NPs-induced increases were significantly attenuated. This significant protective activity can be attributed to the direct scavenging action of free radicals by WGO, thereby disrupting the chain reactions of LPO. In addition, the bioactive compounds present in WGO can help stabilize the cell membrane structure and boost the body's antioxidant defense system. These results confirm the earlier study that showed WGO can inhibit LPO, thereby reducing oxidative stress in xenobiotic-induced tissue damage **(El-Bana et al., 2022; Akool, 2015)**. Although the free and nanoencapsulated WGO formulations showed potent protective activity against LPO, the nanoencapsulated WGO showed better efficacy than the free WGO. This difference was particularly significant in the high-dose TiO_2 NPs exposure. This may be attributed to the optimized pharmacokinetic profile of the WGO-NLC, which protects the bioactive compounds of WGO from degradation by gastric enzymes and first-pass metabolism, thus maximizing its bioavailability. In addition, the encapsulation of WGO by NLC can facilitate its delivery to the site of action through the process of endocytosis, where it can be released to the ER membrane, thereby reaching the site of ROS production. This can be attributed to its potent antioxidant activity, which can be sustained longer than the free WGO, thereby protecting the cell membrane against MDA formation. This confirms the benefits

of using NPs in the delivery system, which can be particularly advantageous in attenuating xenobiotic-induced oxidative **(Gunawan and Boonkanokwong, 2024; Viegas et al., 2023).**

3.4.2.4 Nitric oxide level

Nitric oxide (NO), a key signaling molecule, has the potential to react with reactive oxygen species (ROS) in the context of oxidative stress and produce highly reactive nitrogen species (RNS), thereby increasing the severity of cellular damage and inflammatory responses. The administration of TiO_2 nanoparticles caused a significant increase in the concentration of NO in both hepatic and renal tissues in a dose-dependent manner; the renal tissue was found to be the most responsive organ to the administration of TiO_2 nanoparticles Fig. 6b. Under such conditions of oxidative stress, the elevated concentration of NO has the potential to produce RNS with ROS, thereby increasing the severity of cellular damage and inflammatory responses. The significant increase in the concentration of NO reflects the toxicological effects of the bioaccumulation of TiO_2 nanoparticles in the body. These results confirm the earlier studies carried out by our research group **(Sallam et al., 2023; Rizk et al., 2017)** with regard to the hepatotoxic effects of TiO_2 nanoparticles on the homeostasis of NO.

Even though renal tissues show strong oxidative responses, it has been well demonstrated that the liver has the potential to act as the primary and more vulnerable target organ after the administration of TiO_2 nanoparticles. This vulnerability of the liver is due to the fact that the liver plays an important role in the sequestration, biotransformation, and immune surveillance of nanoparticles, which results in the generation of oxidative and nitrosative stress greater than that occurring in the kidneys as mentioned previously in **(Brand et al., 2020)**. Additionally, the high lipid content in the liver, coupled with a substantial level of polyunsaturated fatty acids (PUFAs) in the hepatocyte membrane, makes these cells particularly vulnerable to injury through lipid peroxidation. The presence of several double bonds in PUFAs makes them highly susceptible to free radicals, thereby increasing the rate of chain lipid peroxidation in the cell membrane, which impairs cellular homeostasis, oxidative injury and increased level of reactive oxygen or nitrogen species. Finally, the immunologic role of the liver may also contribute to increased damage **(Shakeel et al., 2016)**. The activation of Kupffer cells by TiO_2 nanoparticles leads to the release of pro-inflammatory cytokines such as TNF-α and IL-6 and inducible nitric oxide synthase, resulting in increased levels of nitric oxide that cause lipid peroxidation **(Abbasi-Oshaghi et al., 2019)**. In this case, rather than protecting the body from damage, the liver may experience earlier and more complex oxidative and inflammatory injury, making it a major factor that determines toxicity.

In a similar context, the simultaneous administration of free and nano-encapsulated WGO significantly reduced the concentration of NO induced by the administration of TiO_2 nanoparticles in both hepatic and renal tissue homogenates, indicating a protective role against oxidative stress and nitrosative stress. These results are in accordance with earlier studies that demonstrated the potential of WGO to inhibit the synthesis of NO in the context of xenobiotic-induced oxidative stress and to reduce oxidative stress **(El-Bana et al., 2022; Abdallah and Bakry, 2014b)**. Of significant interest was the finding that the efficacy

of the nano-encapsulated form of WGO was higher than that of the free form of the oil in reducing the concentration of NO induced by the administration of TiO_2 nanoparticles, as was previously established.

Genotoxicity

For instance, overproduction of reactive oxygen species (ROS) is a well-established cause of oxidative damage to crucial macromolecules in cells, such as DNA, which is a well-established hallmark of TiO_2 nanoparticle-induced toxicity **(Caoet al., 2023)**. ROS has also been implicated in direct damage to phosphodiester bonds in DNA, which could lead to DNA damage and initiate carcinogenesis **(Akool, 2019)**. In this context, the extent of DNA breakage can be used as a direct measure of TiO_2 nanoparticle-induced genotoxicity. As depicted in Fig. 6c, TiO_2 NPs induced a significant increase in the percentage of DNA breakage in both liver and kidney homogenate samples compared with controls in a dose-dependent manner. This genotoxicity of TiO_2 NPs is in accordance with previous studies showing accumulation of titanium in both liver and kidney tissues **(Zhanget al., 2024; Salmanet al., 2021; Hanet al., 2020).** Significantly, the concomitant use of WGO in its free and nanoencapsulated forms was seen to reduce the DNA damage induced by TiO_2 NPs, as clearly depicted in Fig. 6c. At the lower dose of TiO_2 NPs, the percentages of DNA breakage in the liver and kidney tissues were significantly reduced, showing levels comparable to those of the control. Most impressively, the WGO, as well as its nanoencapsulated form, showed significant genoprotection against the DNA damage induced by the high dose of TiO_2 NPs. This significant genoprotective activity may be attributed to the antioxidant activity of the WGO, which may act by scavenging free radicals, thereby reducing oxidative stress, which leads to DNA damage, as well as supporting DNA repair, maintaining the integrity of the mitochondrial membrane through the action of unsaturated fatty acids, as previously reported **(Akool, 2015)**. Interestingly, in all doses of TiO_2 NPs, the nanoencapsulated form of WGO showed better efficacy in preventing DNA breakage compared to its free form, as indicated by lower percentages of DNA breakage.

Antioxidants enzymes in tissue homogenates

Moreover, it is essential to evaluate the antioxidant potential in the liver and kidneys for assessing oxidative stress caused by xenobiotics. The antioxidant defense mechanism consists of a series of enzyme-catalyzed reactions: Superoxide dismutase (SOD) reduces superoxide radicals to H2O2, which is further converted to H_2O and O_2 by either Catalase (CAT) or Glutathione peroxidase (GPx). The latter depends on a constant availability of reduced Glutathione (GSH), which is recycled from its oxidized form by Glutathione Reductase (GR). Besides these antioxidants enzyme-catalyzed radical-scavenging mechanisms, Glutathione S-transferase (GST) is also involved in xenobiotic detoxification by conjugating GSH with electrophilic compounds, thereby terminating their biological activity and promoting excretion. The antioxidant defense mechanism maintains redox balance and inhibits the formation of potentially harmful compounds **(Hasb Elnabi et al., 2023)**. Figure 7 results indicate that exposure to TiO_2 NPs causes a considerable, concentration-dependent reduction in cellular antioxidant potential in liver and kidney tissue homogenates. There is a considerable reduction in SOD and CAT enzyme activity, as well

as a generalized depression in the glutathione antioxidant pathway, encompassing GR, GST, GPx, and GSH levels in both tissues. The findings are consistent with previous reports **(Zhang et al., 2024; Vasantharaja et al., 2019; Azim et al., 2015)**. The high degree of antioxidant depletion might be due to a high oxidative stress burden caused by TiO_2 NPs, which overwhelms antioxidant defenses by increasing ROS levels beyond antioxidant defenses and disrupting cellular detoxification mechanisms **(Wani et al., 2021; Abdou et al., 2019)**. Moreover, direct interaction with enzyme structures might also play a role. Computational docking analysis by **(Ranjan et al., 2018)** showed that TiO_2 NPs have high affinity for essential amino acids with strongly negative binding energy residues. Where, preferential adhesion occurs at positively charged (Lysine) and nonpolar aliphatic (Proline, Leucine) residues near the active site. This interaction may trigger conformational changes or sterically hinder substrate access resulting in loss of endogenous antioxidant potential. In this context, the synergy between this physical binding and ROS-mediated insult may possibly explain the comprehensive collapse of the antioxidant defense system.

The mechanistic driving force of this endogenous antioxidant system collapse is likely the persistent 'oxidative burst' generated by TiO_2 NPs. The high toxic free radical burden, overwhelms the catalytic capacity of SOD, leading to its functional exhaustion and the subsequent failure of CAT and GPx. This 'redox collapse' explains the sharp decline in GSH levels; as GSH is rapidly consumed to neutralize ROS or conjugated by GST (a compensatory upregulated Phase II detoxification response) to detoxify nanoparticle-derived free radicals and consequently, the GR enzyme becomes unable to keep pace with the demand for GSH recycling. This localized redox failure in the lung and spleen likely mirrors pathological events in the liver and kidneys. The observed depletion of GSH in pulmonary and splenic tissues suggests a state of systemic glutathione bankruptcy, where the liver's biosynthetic capacity) the liver is responsible for the majority of systemic GSH synthesis) is overwhelmed by the oxidative load of circulating TiO_2 NPs.

Co-administration of free or nanoencapsulated WGO significantly mitigated hepatic and renal antioxidant depletion, though its efficacy was organ and antioxidant system-specific. Nanoencapsulated WGO continued to demonstrate a generally superior protective efficacy over the free oil with respect to the glutathione cascade. SOD and CAT activities were successfully maintained near control levels at lower TiO_2 dose, agreeing with previous reported data **(Hafez et al., 2019; Akool, 2015; Hussein et al., 2014)**. However, the glutathione-related cascade (GR, GST, GPx, and GSH) exhibited persistent dysregulation although significantly enhanced in comparison to the respective TiO_2 NPs group. This discrepancy suggests that WGO’s effectively protected the enzymes from structural and oxidative modification (SOD and CAT) but the overwhelming ROS burden kinetically outpaces the regenerative capacity of GR and the conjugative demands of GST, leading to a depletion of the GSH pool and consequently the functional collapse of the glutathione-related cascade specifically under high TiO_2 NPs dose.

Histopathological finding

3.4.2.4.3 Liver histology

The histopathological examination of liver sections Fig. 8 serves as a visual record of the dose-dependent metabolic and structural failure induced by TiO_2 NPs. Exposure to low TiO_2 NPs dose resulted in lobular infiltration by leukocytes and inflammatory cells (L), a cellular response likely triggered by the elevated Nitric Oxide (NO) levels and subsequent pro-inflammatory signaling. The presence of hyperchromatic and vacuolated nuclei indicates significant membrane instability which correlates with the increased MDA level through lipid peroxidation. With the loss of hepatocyte membrane integrity, the intracellular enzymes leak into the systemic circulation, explaining the clinical reduction in AST/ALT ratio.

In addition, the light basophilic cytoplasm suggests a disruption of the metabolic signaling pathways of the liver, which are linked to the endoplasmic reticulum and the mitochondria. These findings are consistent with the alterations observed in the serum glucose and lipid profiles, suggesting a compromised ability of the liver to store glycogen. Moreover, the toxicity of TiO_2 NP was increased in the high-dose cohort, with the liver displaying severe degenerative changes that progressed from reversible to irreversible damage, including necrosis and fibrotic transformation. The presence of pyknotic and necrotic nuclei indicates the failure of metabolic activities, as indicated by the deactivation of the cytochrome P450 system, as well as the antioxidant system, with the depletion of glutathione (GSH) levels and the inactivation of SOD/CAT, thereby permitting the action of ROS to damage DNA and proteins. Importantly, the microscopic visualization of Ti deposits in the lumen of arteries offers a direct corollary to the ICP-OES bioaccumulation results. These Ti deposits are apparently sites of localized damage, as indicated by the marked proliferative activity of the hepatocytes, as well as the onset of fibrotic remodeling, as observed in the fibrotic tissue adjacent to the portal tracts. These findings align with **(Zhang et al., 2024; Hasb Elnabi et al., 2023; Doudi and Setorki, 2015)** who reported similar TiO_2 NPs-induced hepatic lesions such as vacuolated hepatocytes, vascular congestion, dilated sinusoids, degeneration, apoptosis, hepatocellular hypertrophy, lobular effacement, and lamellar necrosis.

The prophylactic co-administration of WGO, particularly as a nanostructured lipid carrier, showed an extensive ability to stop the cascade of oxidative stress while protecting the multifaceted functional integrity of the liver from the toxicity of TiO_2 nanoparticles. While free WGO offered partial architectural preservation, the nanoencapsulated WGO maintained near-total structural and metabolic homeostasis. Microscopically, this was evidenced by the successful preservation of the classic "radiated array" of hepatocytes and the maintenance of narrow, healthy sinusoids, even in the presence of titanium bioaccumulation. Abundant healthy nuclei and prominent nucleoli signify that nanoencapsulated WGO proactively shield protein-synthetic organelles, evident from the observed sustaining of Cytochrome P450, maintaining serum albumin and total protein results and while preventing the accumulation of serum bilirubin. Furthermore, protection of mitochondrial and endoplasmic reticulum (ER) integrity allowed for the uninterrupted preservation of glucose and cholesterol metabolic balance. Furthermore, protection of mitochondrial and endoplasmic reticulum (ER) integrity allowed for the uninterrupted maintenance of glucose and cholesterol homeostasis.

In addition, the structural preservation by nanoencapsulated WGO is the fundamental reason for the stability of the serum biomarkers. By providing antioxidant protection to the hepatocyte membranes, the

nanoencapsulated WGO prohibited LPO-induced membrane rupture, thereby preventing the leakage of AST and ALT into the systemic circulation. This protection not only scavenges free radicals and nitric oxide before they can trigger pro-inflammatory signaling but also prevents the genotoxic "pyknotic" nuclear shifts associated with DNA fragmentation. The technical superiority of the nanoencapsulated WGO confirms the proposed optimized delivery and local high sustained intracellular concentrations of its phytoconstituents directly at the primary sites of ROS generation. Ultimately, WGO-NLCs provide a potent protective microenvironment that suppresses pro-fibrotic inflammatory pathways at their inception, thereby preserving Phase II detoxification capacity and overall hepatic redox homeostasis. This protective effect is consistent with **(Sliai, 2015)** who observed WGO's ability to diminish doxorubicin-induced hepatocyte apoptosis and lipid peroxidation.

Kidney histology

The histopathological examination of renal cortex sections Fig. 9 has provided an insight into the structural basis of renal damage caused by TiO_2 NPs, depending on the administered dose, as observed in this study. When subjected to a low dose of TiO_2 NPs, there was a marked degenerative alteration of the kidney, as evidenced by glomerular atrophy and compensatory increase of urinary space. These changes are directly related to the observed increase of serum levels of urea and creatinine, as a result of compromised glomerular filtration rate due to decreased glomerular filtration surface area. Moreover, the observed presence of hyaline casts within disorganized proximal tubules and dilation of renal tubular lumina are indicative of an early defect of reabsorptive capacity, as observed in this study, and are associated with increased levels of renal lipid peroxidation. The latter occurs as a result of degradation of renal tubular epithelial cell membrane, leading to protein leakage and cast formation, as observed within kidney sections.

When subjected to a high dose of TiO_2 NPs, marked structural damage of renal tissue was observed, leading to severe forms of degenerative nephrotoxicity, as observed in this study. It was noted that the presence of titanium (Ti) within interstitial renal tissue, as observed through ICP-OES, plays a crucial role in initiating localized inflammation and nitrosative stress, as observed through histopathological examination of kidney sections, where cells of renal tubular epithelium and hyaline casts are indicative of terminal forms of oxidative damage, where depletion of renal antioxidant defenses, such as GSH and SOD, allows ROS to cause cellular death, leading to renal failure, as observed through histopathological examination of kidney sections, where glomerular hyperemia and reduction of mesangial cells are indicative of compromised renal function, leading to renal failure, as observed through histopathological examination of kidney sections. These histopathological changes are consistent with those observed by **(Javaheri et al., 2023; Salem et al., 2017)**.

The co-administration of WGO, especially when it was given as a nano-encapsulated formulation, showed a potent ability to arrest the oxidative cascade induced by TiO_2 NPs and preserve renal structural and functional integrity. Indeed, WGO functioned as a preventive shield that maintained the renal glomerular and convoluted tubular structures even when there was significant exposure to TiO_2

NPs. In the WGO-NLC group, the preservation of organized glomerular structures with narrow urinary spaces indicative of healthy glomerular function suggests that this formulation protected the sensitive podocyte and membrane structures of the glomeruli from TiO_2 NPs-induced damage. Presumably, this was the main reason why serum levels of urea and creatinine remained at near-control levels, as this was due to an unimpaired renal excretory function. The greater prophylactic potential of WGO-NLC compared to free WGO can be explained by the fact that it was more effective in delivering this compound, thus maximizing its intracellular concentration at the main sites of TiO_2 NPs-induced damage. This protective effect was visually demonstrated as the virtual absence of tubular necrosis and hyaline cast formation observed in the WGO-NLC co-administered group. By early scavenging ROS and NO, the nano-formulation successfully bypassed the lipid peroxidation cascade, precluding the epithelial desquamation and tubular dilation that underpin renal functional collapse. Moreover, the structural preservation of mesangial cells and the organization of the proximal and distal tubules highlight the protection of the renal filtration and reabsorptive structural and functional integrity evident by the effective retention of serum total protein and albumin, and prevention of the systemic accumulation of bilirubin. This protective effect aligns with **(El-Bana et al., 2022; Hafez et al., 2019)** where they demonstrated the ability of WGO to mitigate gentamicin and cisplatin-induced nephrotoxicity by reducing inflammation, fibrosis, and degenerative changes, ultimately restoring kidney structure.

Immunohistochemical finding

The immunohistochemical analysis of hepatic and renal tissues Fig. 10**and** Fig. 11 provides a molecular basis for the architectural and metabolic failure observed following TiO_2 NPs exposure. As a primary signaling molecule in the innate immune response, TNF-α plays a pivotal role in translating localized oxidative stress into systemic inflammatory damage and tissue degeneration, the change in the levels of pro-inflammatory cytokines such as TNF-α has crucial roles within tissue injury, and a broad range of renal tissues, including immune cells, mesangial cells, glomeruli, tubular epithelial cells, and endothelial cells **(Zhanget al., 2007).** While GP88 is a granulin precursor protein of the endoplasmic reticulum involved in cellular homeostasis, its pathological upregulation is a hallmark of oxidative stress and tissue injury **(Arechavaleta-Velascoet al., 2017)**, it has shown many biological effects such as cellular proliferation **(Hoet al., 2008)**, its overexpression in tissues was increased in biological fluids observed in many different liver diseases **(Cheunget al., 2014; Cheunget al., 2011)**. In the present study, an intense, dark brown granules indicative of TNF-α overexpression were observed in the high level TiO_2 NPs exposure group. This upregulated expression in comparison to control correlate directly with the observed surge in tissue nitric oxide levels and the extensive leukocyte infiltration observed in histology study. As a master pro-inflammatory cytokine, the upregulation of TNF-α triggers a cascade of oxidative stress and lipid peroxidation, which fundamentally compromises cell membrane integrity and providing a possible molecular explanation that for the observed clinical rise in serum transaminases (AST and ALT) and renal markers (urea and creatinine). In addition, the dark cytoplasmic granules of GP88 in the high level TiO_2 NPs exposure group aligns with the observed inactivation of the Cytochrome P450 system and the decline in serum albumin. These findings are consistent with established models where TiO_2 NPs

bioaccumulation triggers chronic inflammation and fibrotic remodeling **(Abbasi-Oshaghiet al., 2019; Morganet al., 2017a; Morganet al., 2017b)**. Furthermore, The investigations of **(Basaket al., 2025)** revealed that titanium dioxide exposure caused notable kidney tissue damage with increased apoptosis (caspase-3), elevated oxidative stress (strong 4-HNE staining) and inflammatory markers TNF-α and IL-6.

The prophylactic co-administration of WGO-NLCs showed an overall potential to block inflammatory signaling before it manifests as structural damage. When compared with the high-dose TiO_2 NP exposure group, it was observed that, unlike the rats treated with TiO_2 NPs, the rats treated with nanoencapsulated WGO showed pale, weak immunostaining for both TNF-α and GP88, a finding that was strikingly similar to that of the control group. The prevention of upregulation of these molecular markers has shown that WGO-NLCs have effectively neutralized the initial onset of ROS/RNS, thus preventing the “alarm” signaling that would otherwise trigger an overproduction of cytokines. By keeping TNF-α and GP88 at baseline levels, WGO-NLCs have prevented the onset of an oxidative cascade that would otherwise lead to lipid peroxidation, thus resulting in membrane damage. These protective mechanisms at the molecular level have, therefore, contributed to the preservation of hepatic and renal glucose, lipid, and protein profiles. Moreover, prevention of GP88-mediated pathways that lead to chronic damage has shown that WGO-NLCs have successfully inhibited pathways that would otherwise lead to irreversible damage of the liver and kidneys. These findings have shown that, due to better delivery and intracellular concentration, WGO-NLCs have provided a robust prophylactic shield that has ensured that hepatic and renal metabolic activity remains functional and structurally intact.

3.4.4 Conclusion

This study assessed the therapeutic potential of wheat germ oil, a powerful antioxidant, in its native as well as nanoencapsulated forms, for the treatment of dose-dependent hepatorenal toxicity caused by titanium dioxide nanoparticles. Intraperitoneal injection of TiO_2 NPs over a period of six weeks resulted in severe liver and kidney damage, as indicated by increased levels of serum urea, creatinine, total proteins, and liver enzymes, along with decreased levels of uric acid. These changes were associated with increased levels of titanium in liver and kidney tissues, where severe oxidative stress, as indicated by increased levels of malondialdehyde, decreased levels of glutathione, and decreased activities of antioxidant enzymes SOD and CAT, had developed. Histopathological examination of liver and kidney tissues showed severe inflammation, necrosis, apoptosis, and fibrosis, along with increased levels of inflammatory biomarker TNF-alpha, as well as stress biomarker GP88. WGO, particularly in its nanoencapsulated form, significantly reduced these changes. WGO helped remove the accumulated titanium from tissues, restoring antioxidant balance. The increased efficacy of WGO in its nanoencapsulated form might be due to its better delivery, uptake, and modulation of antioxidant balance through its free radical scavenging activity. In addition, no significant changes were observed in the free WGO, nanoencapsulated WGO, and Placebo groups, as compared to the control group, indicating the safety of WGO as well as the nanoencapsulating system. The absence of toxicity in the placebo

group is particularly noteworthy, as it indicates that the lipid, polymer, as well as the surfactant, components of the nanoencapsulating system have no adverse effects.

Recommendation

Based on the present findings, titanium dioxide nanoparticles should be used with caution and responsibility, their application must follow strict safety regulations, especially in food, cosmetics. Moreover, nanoencapsulated wheat germ oil is recommended as a promising protective and therapeutic strategy against titanium dioxide nanoparticle–induced hepatorenal toxicity. Future studies should focus on long-term safety assessment, detailed molecular mechanisms, and dose optimization. Additionally, translational investigations and controlled clinical studies are warranted to evaluate its potential application in occupational, environmental, and food-related nanoparticle exposure scenarios.

Declarations

Declaration of competing interest

The authors declare that they have no known competing financial interests or personal relationships that could have appeared to influence the work reported in this paper.

Funding

The authors did not receive support from any organization for the submitted work.

Author Contribution

Nagat D. Kotba: Conceptualization, methodology, Formal analysis, writing original draft preparation, and writing review and editing.Mai M. Ali: Supervision, Investigation, data collection, Formal analysis, and writing original draft preparation.Marium M. Shamaa: Formal analysis, data curation, and visualization.Mona A.H. Yehia: Methodology, histology, and immunohistochemical studies.Sabah G. El-Banna: Supervision, investigation, Formal analysis, and data collectionAll authors have read and approved the final version of the manuscript.

Acknowledgement

This work is dedicated to the memory of late supervisor, Prof. Dr. Hesham Zaki Ibrahim. His mentorship, wisdom, and unwavering dedication to science continue to inspire my work and will always be remembered with deep respect and gratitude.

Data Availability

Data available upon request

References

1. Abbasi-Oshaghi, E., Mirzaei, F., & Pourjafar, M. (2019). NLRP3 inflammasome, oxidative stress, and apoptosis induced in the intestine and liver of rats treated with titanium dioxide nanoparticles: in vivo and in vitro study. *International journal of nanomedicine*, 1919–1936.
2. Abdallah, A., & Bakry, S. (2014a). Hepatoprotective and Antioxidant Activity of Wheat Germ Oil Against Nicotine Induced Oxidative Stress. *Advances in Biological Research, 8*(6), 289–297.
3. Abdallah, A. A. M., & Bakry, S. (2014b). *Hepatoprotective and Antioxidant Activity of Wheat Germ Oil Against Nicotine Induced Oxidative Stress*.
4. Abdel-Halim, K. Y., Osman, S. R., Abuzeid, M. A., El-Danasoury, H. T., & Khozimy, A. M. (2022). Apoptotic and histopathological defects enhanced by titanium dioxide nanoparticles in male mice after short-term exposure. *Toxicology Reports, 9*, 1331–1346.
5. Abdou, K., Moselhy, W. A., Mohamed, H. M., El-Nahass, E.-S., & Khalifa, A. G. (2019). Moringa oleifera leaves extract protects titanium dioxide nanoparticles-induced nephrotoxicity via Nrf2/HO-1 signaling and amelioration of oxidative stress. *Biological Trace Element Research, 187*, 181–191.
6. Abuzaied, H., Bashir, D. W., Rashad, E., Rashad, M. M., & El-Habback, H. (2024). Ginseng Extract can alleviate The Induced-renal Toxicity of Titanium Dioxide Nanoparticles in a Rat Model. *Journal of Applied Veterinary Sciences, 9*(2), 1–17.
7. Aibani, N., Rai, R., Patel, P., Cuddihy, G., & Wasan, E. K. (2021). Chitosan nanoparticles at the biological interface: implications for drug delivery. *Pharmaceutics, 13*(10), 1686.
8. Ajiboye, A. L., Nandi, U., Galli, M., & Trivedi, V. (2021). Olanzapine loaded nanostructured lipid carriers via high shear homogenization and ultrasonication. *Scientia Pharmaceutica, 89*(2), 25.
9. Akool, E.-S. (2015). Molecular mechanisms of the protective role of wheat germ oil against cyclosporin A-induced hepatotoxicity in rats. *Pharmaceutical biology, 53*(9), 1311–1317.
10. Akool, E.-S. (2019). Molecular mechanisms of the protective role of wheat germ oil against oxidative stress–induced liver disease *Dietary interventions in liver disease* (pp. 233–238): Elsevier.
11. Alamery, S., Zargar, S., Yaseen, F., Wani, T. A., & Siyal, A. (2022). Evaluation of the effect of wheat germ oil and olmutinib on the thioacetamide-induced liver and kidney toxicity in mice. *Life, 12*(6), 900.
12. Alidadi, H., Khorsandi, L., & Shirani, M. (2018). Effects of quercetin on tubular cell apoptosis and kidney damage in rats induced by titanium dioxide nanoparticles. *The Malaysian Journal of Medical Sciences: MJMS, 25*(2), 72.
13. ANI, A., Ani, M., MOSHTAGHI, S. A. A., & Ahmadvand, H. (2008). Changes in liver contents of lipid fractions following titanium exposure.

14. Apostolou, M., Assi, S., Fatokun, A. A., & Khan, I. (2021). The effects of solid and liquid lipids on the physicochemical properties of nanostructured lipid carriers. *Journal of pharmaceutical sciences, 110*(8), 2859–2872.
15. Arechavaleta-Velasco, F., Perez-Juarez, C. E., Gerton, G. L., & Diaz-Cueto, L. (2017). Progranulin and its biological effects in cancer. *Medical Oncology, 34*(12), 194.
16. Assmann, G., Jabs, H.-U., Kohnert, U., Nolte, W., & Schriewer, H. (1984). LDL-cholesterol determination in blood serum following precipitation of LDL with polyvinylsulfate. *Clinica chimica acta, 140*(1), 77–83.
17. Azim, S. A. A., Darwish, H. A., Rizk, M. Z., Ali, S. A., & Kadry, M. O. (2015). Amelioration of titanium dioxide nanoparticles-induced liver injury in mice: possible role of some antioxidants. *Experimental and Toxicologic Pathology, 67*(4), 305–314.
18. Barham, D., & Trinder, P. (1972). An improved colour reagent for the determination of blood glucose by the oxidase system. *Analyst, 97*(1151), 142–145.
19. Basak, F., Kusat, T., Kahraman, T., & Ersan, Y. (2025). The role of resveratrol in delivering antioxidant, anti-inflammatory, and anti-apoptotic defense against nephrotoxicity generated by titanium dioxide. *Naunyn-Schmiedeberg's Archives of Pharmacology*, 1–13.
20. Bashiri, S., Ghanbarzadeh, B., Ayaseh, A., Dehghannya, J., & Ehsani, A. (2020). Preparation and characterization of chitosan-coated nanostructured lipid carriers (CH-NLC) containing cinnamon essential oil for enriching milk and anti-oxidant activity. *Lwt, 119*, 108836.
21. Belfield, A., & Goldberg, D. (1971). Revised assay for serum phenyl phosphatase activity using 4-amino-antipyrine. *Enzyme, 12*(5), 561–573.
22. Boughediri, K., Ouazouaz, M., Triki, R., & Henchiri, C. (2024). The therapeutic potential of saharian monovarietal virgin olive oil (olea europea l.) on hematological, histological, and antioxidant status in titanium dioxide nanoparticles-induced oxidative stress in rats. *Comparative Clinical Pathology, 33*(3), 411–423.
23. Boutillier, S., Fourmentin, S., & Laperche, B. (2022). History of titanium dioxide regulation as a food additive: a review. *Environmental Chemistry Letters*, 1–17.
24. Brand, W., Peters, R. J., Braakhuis, H. M., Maślankiewicz, L., & Oomen, A. G. (2020). Possible effects of titanium dioxide particles on human liver, intestinal tissue, spleen and kidney after oral exposure. *Nanotoxicology, 14*(7), 985–1007.
25. Bucolo, G., & David, H. (1973). Quantitative determination of serum triglycerides by the use of enzymes. *Clinical chemistry, 19*(5), 476–482.
26. Cao, Y., Chen, J., Bian, Q., Ning, J., Yong, L., Ou, T., Song, Y., & Wei, S. (2023). Genotoxicity evaluation of titanium dioxide nanoparticles in vivo and in vitro: A meta-analysis. *Toxics, 11*(11), 882.
27. Chang, H., Li, L., Deng, Y., Song, G., & Wang, Y. (2023). Protective effects of lycopene on TiO2 nanoparticle-induced damage in the liver of mice. *Journal of applied toxicology, 43*(6), 913–928.
28. Chen, Z., Zhou, D., Zhou, S., & Jia, G. (2019). Gender difference in hepatic toxicity of titanium dioxide nanoparticles after subchronic oral exposure in Sprague-Dawley rats. *Journal of applied toxicology,*

39(5), 807–819.

29. Cheung, P. F., Yip, C. W., Wong, N. C., Fong, D. Y., Ng, L. W., Wan, A. M., Wong, C. K., Cheung, T. T., Ng, I. O., & Poon, R. T. (2014). Granulin–epithelin precursor renders hepatocellular carcinoma cells resistant to natural killer cytotoxicity. *Cancer immunology research, 2*(12), 1209–1219.
30. Cheung, P. F. Y., Cheng, C. K. C., Wong, N. C. L., Ho, J. C. Y., Yip, C. W., Lui, V. C. H., Cheung, A. N. Y., Fan, S. T., & Cheung, S. T. (2011). Granulin-epithelin precursor is an oncofetal protein defining hepatic cancer stem cells. *PloS one, 6*(12), e28246.
31. Contreras-Zentella, M. L., & Hernández-Muñoz, R. (2016). Is liver enzyme release really associated with cell necrosis induced by oxidant stress? *Oxidative medicine and cellular longevity, 2016*(1), 3529149.
32. Dachev, M., Bryndová, J., Jakubek, M., Moučka, Z., & Urban, M. (2021). The effects of conjugated linoleic acids on cancer. *Processes, 9*(3), 454.
33. de Sousa, D. P., de Assis Oliveira, F., Arcanjo, D. D. R., da Fonsêca, D. V., Duarte, A. B. S., de Oliveira Barbosa, C., Ong, T. P., & Brocksom, T. J. (2024). Essential Oils: Chemistry and Pharmacological Activities—Part II. *Biomedicines, 12*(6), 1185.
34. Dhupal, M., Oh, J.-M., Tripathy, D. R., Kim, S.-K., Koh, S. B., & Park, K.-S. (2018). Immunotoxicity of titanium dioxide nanoparticles via simultaneous induction of apoptosis and multiple toll-like receptors signaling through ROS-dependent SAPK/JNK and p38 MAPK activation. *International journal of nanomedicine*, 6735–6750.
35. DM, G. (1983). Assay of glutathione reductase. *Methods in enzymatic analysis*.
36. Doudi, M., & Setorki, M. (2015). Influence of titanium dioxide nanoparticles on oxidative stress and pulmonary dysfunction. *Zahedan Journal of Research in Medical Sciences, 17*(9).
37. Doumas, B. T., Watson, W. A., & Biggs, H. G. (1971). Albumin standards and the measurement of serum albumin with bromcresol green. *Clinica chimica acta, 31*(1), 87–96.
38. Eilola, K., & Perämäki, P. (2001). Microwave heated vapor-phase digestion method for biological sample materials. *Fresenius' journal of analytical chemistry, 369*(1), 107–112.
39. El-Bana, M. A., Abdelaleem, A. H., El-Naggar, M. E., Farrag, A. H., Mohamed, S. M., & El-Khayat, Z. (2022). Formulation of wheat germ oil based on nanoemulsions to mitigate cisplatin's nephrotoxic effects. *Prostaglandins & Other Lipid Mediators, 158*, 106603.
40. El-Nashar, H. A., Abbas, H., Zewail, M., Noureldin, M. H., Ali, M. M., Shamaa, M. M., Khattab, M. A., & Ibrahim, N. (2022). Neuroprotective effect of artichoke-based nanoformulation in sporadic Alzheimer's disease mouse model: focus on antioxidant, anti-inflammatory, and amyloidogenic pathways. *Pharmaceuticals, 15*(10), 1202.
41. Ellman, M. (1959). A spectrophotometric method for determination of reduced glutathione in tissues. *Anal Biochem, 74*(1), 214–226.
42. Emam, K. K., Abdel Fattah, M. E., El Rayes, S. M., Hebishy, M. A., & Dessouki, A. A. (2022). Assessment of wheat germ oil role in the prevention of induced breast cancer in rats. *ACS omega, 7*(16), 13942–13952.

43. Fadda, L. M., Hagar, H., Mohamed, A. M., & Ali, H. M. (2018). Quercetin and idebenone ameliorate oxidative stress, inflammation, DNA damage, and apoptosis induced by titanium dioxide nanoparticles in rat liver. *Dose-Response, 16*(4), 1559325818812188.
44. Fatemeh, M. F., & Mohammad, F. (2014). The histological and biochemical effects of titanium dioxide nanoparticle (TiO2) on the liver in wistar Rat. *Int res j boil sci, 3*, 2278–3202.
45. Festing, M. F., & Altman, D. G. (2002). Guidelines for the design and statistical analysis of experiments using laboratory animals. *ILAR journal, 43*(4), 244–258.
46. Frings, C. S., Fendley, T. W., Dunn, R. T., & Queen, C. A. (1972). Improved determination of total serum lipids by the sulfo-phospho-vanillin reaction. *Clinical chemistry, 18*(7), 673–674.
47. Fröhlich, E., Kueznik, T., Samberger, C., Roblegg, E., Wrighton, C., & Pieber, T. R. (2010). Size-dependent effects of nanoparticles on the activity of cytochrome P450 isoenzymes. *Toxicology and applied pharmacology, 242*(3), 326–332.
48. Ghagane, S. C., Puranik, S. I., Kumbar, V. M., Nerli, R. B., Jalalpure, S. S., Hiremath, M. B., Neelagund, S., & Aladakatti, R. (2017). In vitro antioxidant and anticancer activity of Leea indica leaf extracts on human prostate cancer cell lines. *Integrative medicine research, 6*(1), 79–87.
49. Ghareeb, O. A. (2023). Adverse impact of titanium dioxide nanoparticles on hepato-renal functions and improved role of Rosmarinus officinalis. *Journal of Natural Science, Biology and Medicine, 14*(1), 33–38.
50. Gilani, S. J., Jumah, M. N. b., Zafar, A., Imam, S. S., Yasir, M., Khalid, M., Alshehri, S., Ghuneim, M. M., & Albohairy, F. M. (2022). Formulation and evaluation of nano lipid carrier-based ocular gel system: optimization to antibacterial activity. *Gels, 8*(5), 255.
51. Gunawan, M., & Boonkanokwong, V. (2024). Current applications of solid lipid nanoparticles and nanostructured lipid carriers as vehicles in oral delivery systems for antioxidant nutraceuticals: A review. *Colloids and Surfaces B: Biointerfaces, 233*, 113608.
52. Guo, D., Dou, D., Li, X., Zhang, Q., Bhutto, Z. A., & Wang, L. (2018). Ivermection-loaded solid lipid nanoparticles: preparation, characterisation, stability and transdermal behaviour. *Artificial cells, nanomedicine, and biotechnology, 46*(2), 255–262.
53. Guo, L., Liu, X.-H., Qin, D., Gao, L., Zhang, H., Liu, J.-Y., & Cui, Y. (2009). Effects of nanosized titanium dioxide on the reproductive system of male mice. *Zhonghua nan ke xue= National journal of andrology, 15*(6), 517–522.
54. Habig, W. H., Pabst, M. J., & Jakoby, W. B. (1974). Glutathione S-transferases: the first enzymatic step in mercapturic acid formation. *Journal of biological Chemistry, 249*(22), 7130–7139.
55. Hafez, L. O., Ali, F. A., El-Ghoneimy, A. A., & Abdel-Aziz, M. I. (2019). Nephro-Protective effect of wheat germ oil on gentamicin-induced acute nephrotoxicity in wistar albino rat. *SVU-International Journal of Veterinary Sciences, 2*(1), 51–67.
56. Hamilton, J. S., & Klett, E. L. (2021). Linoleic acid and the regulation of glucose homeostasis: A review of the evidence. *Prostaglandins, Leukotrienes and Essential Fatty Acids, 175*, 102366.

57. Han, B., Pei, Z., Shi, L., Wang, Q., Li, C., Zhang, B., Su, X., Zhang, N., Zhou, L., & Zhao, B. (2020). TiO2 nanoparticles caused DNA damage in lung and extra-pulmonary organs through ROS-activated FOXO3a signaling pathway after intratracheal administration in rats. *International journal of nanomedicine*, 6279–6294.
58. Hasb Elnabi, M. A., Mohamed, S. A., Salman, H. M., Elsayed, H. M., Hashim, M. S., & Said, A. M. (2023). TOXIC EFFECTS OF TITANIUM DIOXIDE NANO-PARTICLES IN ADULT MALE WISTAR RATS LIVER AND THE POSSIBLE PROTECTIVE ROLE OF BETA CAROTENE. *The Egyptian Journal of Forensic Sciences and Applied Toxicology, 23*(2), 45–66.
59. Hassan, D. M., El-Kamel, A. H., Allam, E. A., Bakr, B. A., & Ashour, A. A. (2024). Chitosan-coated nanostructured lipid carriers for effective brain delivery of Tanshinone IIA in Parkinson's disease: interplay between nuclear factor-kappa β and cathepsin B. *Drug Delivery and Translational Research, 14*(2), 400–417.
60. Hassanein, K. M., & El-Amir, Y. O. (2017). Protective effects of thymoquinone and avenanthramides on titanium dioxide nanoparticles induced toxicity in Sprague-Dawley rats. *Pathology-Research and Practice, 213*(1), 13–22.
61. Heller, A., Jarvis, K., & Coffman, S. S. (2018). Association of type 2 diabetes with submicron titanium dioxide crystals in the pancreas. *Chemical Research in Toxicology, 31*(6), 506–509.
62. Heringa, M., Peters, R., Bleys, R., Van Der Lee, M., Tromp, P., Van Kesteren, P., Van Eijkeren, J., Undas, A., Oomen, A., & Bouwmeester, H. (2018). Detection of titanium particles in human liver and spleen and possible health implications. *Particle and fibre toxicology, 15*, 1–9.
63. Ho, J. C., Ip, Y. C., Cheung, S. T., Lee, Y. T., Chan, K. F., Wong, S. Y., & Fan, S. T. (2008). Granulin-epithelin precursor as a therapeutic target for hepatocellular carcinoma. *Hepatology, 47*(5), 1524–1532.
64. Honary, S., & Zahir, F. (2013). Effect of zeta potential on the properties of nano-drug delivery systems-a review (Part 1). *Tropical journal of pharmaceutical research, 12*(2), 255–264.
65. Hu, H., Fan, X., Yin, Y., Guo, Q., Yang, D., Wei, X., Zhang, B., Liu, J., Wu, Q., & Oh, Y. (2019a). Mechanisms of titanium dioxide nanoparticle-induced oxidative stress and modulation of plasma glucose in mice. *Environmental Toxicology, 34*(11), 1221–1235.
66. Hu, H., Li, L., Guo, Q., Zong, H., Yan, Y., Yin, Y., Wang, Y., Oh, Y., Feng, Y., & Wu, Q. (2018). RNA sequencing analysis shows that titanium dioxide nanoparticles induce endoplasmic reticulum stress, which has a central role in mediating plasma glucose in mice. *Nanotoxicology, 12*(4), 341–356.
67. Hu, W., Fitzgerald, M., Topp, B., Alam, M., & O'Hare, T. J. (2019b). A review of biological functions, health benefits, and possible de novo biosynthetic pathway of palmitoleic acid in macadamia nuts. *Journal of Functional Foods, 62*, 103520.
68. Hussein, S. A., Abdel-Aal, S., & Elghwab, A. (2014). Biochemical role of wheat germ oil on biomarkers of oxidative stress and inflammatory response in a rat model of endotoxemia. *Benha Vet Med J, 27*(2), 157–167.

69. Ismael, O. E., Hashish, E. A., & Ali, H. A. (2014). Lipid Profile and Lipogensis Following Corn Oil, Truffle Oil or Wheat Germ Oil Administration in Albino Rat. *Global Veterinaria, 12*(4), 461–469.
70. Javaheri, R., Raji, A. R., Moghaddam Jafari, A., & Nourani, H. (2023). Effects of Oral Exposure to Titanium Dioxide Nanoparticles on the Liver, Small Intestine, and Kidney of Rats assessed by light microscopy and Transmission Electron Microscopy. *Iranian Journal of Veterinary Science and Technology, 15*(1), 41–48.
71. Kaplan, M. M., & Utiger, R. D. (1978). Iodothyronine metabolism in rat liver homogenates. *The Journal of clinical investigation, 61*(2), 459–471.
72. Kato, R., & Gillette, J. R. (1965). Effect of starvation on NADPH-dependent enzymes in liver microsomes of male and female rats. *Journal of Pharmacology and Experimental Therapeutics, 150*(2), 279–284.
73. Khalifa, F. K., Khalil, F. A., Barakat, H. A., & Hassan, M. M. (2011). Protective role of wheat germ and grape seed oils in chlorpyrifos-induced oxidative stress, biochemical and histological alterations in liver of rats.
74. Khan, J., Kim, N. D., Bromhead, C., Truman, P., Kruger, M. C., & Mallard, B. L. (2025). Hepatotoxicity of titanium dioxide nanoparticles. *Journal of applied toxicology, 45*(1), 23–46.
75. Knedel, M., & Böttger, R. (1967). Eine kinetische Methode zur Bestimmung der Aktivität der Pseudocholinesterase (Acylcholin-acylhydrolase 3.1. 1.8.). *Klinische Wochenschrift, 45*, 325–327.
76. Kotil, T., Akbulut, C., & Yön, N. D. (2017). The effects of titanium dioxide nanoparticles on ultrastructure of zebrafish testis (Danio rerio). *Micron, 100*, 38–44.
77. Lash, L. H. (2022). Cellular and functional biomarkers of renal injury and disease. *Current opinion in toxicology, 31*, 100348.
78. Levitt, M. D., Hapak, S. M., & Levitt, D. G. (2022). Alkaline phosphatase pathophysiology with emphasis on the seldom-discussed role of defective elimination in unexplained elevations of serum ALP–a case report and literature review. *Clinical and Experimental Gastroenterology*, 41–49.
79. Li, H., Zhao, X., Ma, Y., Zhai, G., Li, L., & Lou, H. (2009). Enhancement of gastrointestinal absorption of quercetin by solid lipid nanoparticles. *Journal of Controlled Release, 133*(3), 238–244.
80. Liu, C., Sun, Y., Yang, L., Chen, Y., Ji, R., Wang, H., Shi, J., & Wang, J. (2022). The hypolipidemic and antioxidant activity of wheat germ and wheat germ protein in high-fat diet-induced rats. *Molecules, 27*(7), 2260.
81. Manzoor, Q., Sajid, A., Ali, Z., Nazir, A., Sajid, A., Imtiaz, F., Iqbal, S., Younas, U., Arif, H., & Iqbal, M. (2024). Toxicity spectrum and detrimental effects of titanium dioxide nanoparticles as an emerging pollutant: A review. *Desalination and Water Treatment, 317*, 100025.
82. Montgomery, H. (1971). The determination of nitrite in water. *Analyst, 1*, 123–130.
83. Morgan, A., Galal, M. K., Ogaly, H. A., Ibrahim, M. A., Abd-Elsalam, R. M., & Noshy, P. (2017a). Tiron ameliorates oxidative stress and inflammation in titanium dioxide nanoparticles induced nephrotoxicity of male rats. *Biomedicine & Pharmacotherapy, 93*, 779–787.

84. Morgan, A. M., Ibrahim, M. A., & Noshy, P. A. (2017b). Reproductive toxicity provoked by titanium dioxide nanoparticles and the ameliorative role of Tiron in adult male rats. *Biochemical and biophysical research communications, 486*(2), 595–600.
85. Naghshi, S., Aune, D., Beyene, J., Mobarak, S., Asadi, M., & Sadeghi, O. (2021). Dietary intake and biomarkers of alpha linolenic acid and risk of all cause, cardiovascular, and cancer mortality: systematic review and dose-response meta-analysis of cohort studies. *Bmj, 375*.
86. Nagib, R. (2018). Protective effect of wheat germ powder and oil on metabolic disturbances in rats. *Journal of Food and Dairy Sciences, 3*(3), 21–27.
87. Nash, T. (1953). The colorimetric estimation of formaldehyde by means of the Hantzsch reaction. *Biochemical journal, 55*(3), 416.
88. Nishikimi, M., Rao, N. A., & Yagi, K. (1972). The occurrence of superoxide anion in the reaction of reduced phenazine methosulfate and molecular oxygen. *Biochemical and biophysical research communications, 46*(2), 849–854.
89. Norušis, M. J. (2006). *SPSS 14.0 guide to data analysis*: Prentice Hall Upper Saddle River, NJ.
90. Omura, T., & Sato, R. (1964). The carbon monoxide-binding pigment of liver microsomes. I. Evidence for its hemoprotein nature. *J biol Chem, 239*(7), 2370–2378.
91. Orabi, S. H., Abd Eldaim Mabrouk, A., Shawky, S. M., & Zaid, A. (2016). Wheat germ oil ameliorates sucrose induced hepatosteatosis and dyslipidemia through controlling lipogenic and Cholestrogenic genes expression in rats. *Int J Agric Innov Res, 4*(4), 619–626.
92. Orazizadeh, M., Fakhredini, F., Mansouri, E., & Khorsandi, L. (2014). Effect of glycyrrhizic acid on titanium dioxide nanoparticles-induced hepatotoxicity in rats. *Chemico-biological interactions, 220*, 214–221.
93. Paglia, D. E., & Valentine, W. N. (1967). Studies on the quantitative and qualitative characterization of erythrocyte glutathione peroxidase. *The Journal of laboratory and clinical medicine, 70*(1), 158–169.
94. Park, J. H., Jo, Y.-I., & Lee, J.-H. (2020). Renal effects of uric acid: hyperuricemia and hypouricemia. *The Korean journal of internal medicine, 35*(6), 1291.
95. Patton, G., & Crouch, S. (1977). Determination of urea (urease modified Berthelot reaction). *Anal. Chem, 49*, 464–469.
96. Persijn, J. P., & van der Slik, W. (1976). A new method for the determination of gamma-glutamyltransferase in serum. *J Clin Chem Clin Biochem, 14*(9), 421–427. doi: 10.1515/cclm.1976.14.1-12.421
97. Philips, C. A., Augustine, P., Rajesh, S., Ahamed, R., George, T., Padsalgi, G., Paramaguru, R., Valiathan, G., & John, S. K. (2020). Granulocyte colony-stimulating factor use in decompensated cirrhosis: lack of survival benefit. *Journal of Clinical and Experimental Hepatology, 10*(2), 124–134.
98. Price, C. P., Bossuyt, P., & Bruns, D. E. (1976). Tietz fundamentals of clinical chemistry. *Medicine, 3*(1).

99. Prieto, P., Pineda, M., & Aguilar, M. (1999). Spectrophotometric quantitation of antioxidant capacity through the formation of a phosphomolybdenum complex: specific application to the determination of vitamin E. *Analytical biochemistry, 269*(2), 337–341.
100. Priyam, A., Singh, P. P., & Gehlout, S. (2018). Role of endocrine-disrupting engineered nanomaterials in the pathogenesis of type 2 diabetes mellitus. *Frontiers in endocrinology, 9*, 704.
101. Ranjan, S., Dasgupta, N., Sudandiradoss, C., Ramalingam, C., & Kumar, A. (2018). Titanium dioxide nanoparticle–protein interaction explained by docking approach. *International journal of nanomedicine, 13*(sup1), 47–50.
102. Reitman, S., & Frankel, S. (1957). Determination of glutamate-pyruvate transaminase (ALT) and aspartate aminotransfrase (AST). *J Clin Pathol, 28*, 56.
103. Remya, P., & Damodharan, N. (2018). Formulation, development, and characterization of cilnidipine loaded solid lipid nanoparticles. *Asian J Pharm Clin Res, 11*(9), 120–125.
104. Richmond, N. (1973). Colorimetric determination of total cholesterol and high density lipoprotein cholesterol (HDL-c). *Clin. chem, 19*(12), 1350–1356.
105. Rizk, M. Z., Ali, S. A., Hamed, M. A., El-Rigal, N. S., Aly, H. F., & Salah, H. H. (2017). Toxicity of titanium dioxide nanoparticles: effect of dose and time on biochemical disturbance, oxidative stress and genotoxicity in mice. *Biomedicine & Pharmacotherapy, 90*, 466–472.
106. Sacks, F. M., Lichtenstein, A. H., Wu, J. H., Appel, L. J., Creager, M. A., Kris-Etherton, P. M., Miller, M., Rimm, E. B., Rudel, L. L., & Robinson, J. G. (2017). Dietary fats and cardiovascular disease: a presidential advisory from the American Heart Association. *Circulation, 136*(3), e1-e23.
107. Saleh, H. (2016a). Modulatory effect of wheat germ oil on intestinal oxidative stress and DNA damage induced by carbon tetrachloride in Mice. *Journal of Applied Pharmaceutical Science, 6*(12), 067–074.
108. Saleh, H. (2016b). Preventive effect of wheat germ oil on methotrexate–induced liver injury and oxidative intestinal damage in mice. *Journal of Bioscience and Applied Research, 2*(8), 540–548.
109. Salem, M. M., Altayeb, Z. M., & El-Mahalaway, A. M. (2017). Histological and immunohistochemical study of titanium dioxide nanoparticle effect on the rat renal cortex and the possible protective role of lycopene. *Egyptian Journal of Histology, 40*(1), 80–93.
110. Salguero, F., Mekonnen, T., Ruiz-Villamor, E., Sánchez-Cordón, P., & Gómez-Villamandos, J. (2001). Detection of monokines in paraffin-embedded tissues of pigs using polyclonal antibodies. *Veterinary research, 32*(6), 601–609.
111. Sallam, M. F., Ahmed, H. M., Diab, K. A., El-Nekeety, A. A., Abdel-Aziem, S. H., Sharaf, H. A., & Abdel-Wahhab, M. A. (2022). Improvement of the antioxidant activity of thyme essential oil against biosynthesized titanium dioxide nanoparticles-induced oxidative stress, DNA damage, and disturbances in gene expression in vivo. *Journal of Trace Elements in Medicine and Biology, 73*, 127024.
112. Sallam, M. F., Ahmed, H. M., El-Nekeety, A. A., Diab, K. A., Abdel-Aziem, S. H., Sharaf, H. A., & Abdel-Wahhab, M. A. (2023). Assessment of the oxidative damage and genotoxicity of titanium dioxide

nanoparticles and exploring the protective role of holy basil oil nanoemulsions in rats. *Biological Trace Element Research, 201*(3), 1301–1316.

113. Salman, A. S., Al-Shaikh, T. M., Hamza, Z. K., El-Nekeety, A. A., Bawazir, S. S., Hassan, N. S., & Abdel-Wahhab, M. A. (2021). Matlodextrin-cinnamon essential oil nanoformulation as a potent protective against titanium nanoparticles-induced oxidative stress, genotoxicity, and reproductive disturbances in male mice. *Environmental Science and Pollution Research, 28*, 39035–39051.
114. Schirmeister, J. (1964). Determination of creatinine in serum. *Dtsch Med Wschr, 89*(1940), 796.
115. Shakeel, M., Jabeen, F., Qureshi, N. A., & Fakhr-e-Alam, M. (2016). Toxic effects of titanium dioxide nanoparticles and titanium dioxide bulk salt in the liver and blood of male Sprague-Dawley rats assessed by different assays. *Biological Trace Element Research, 173*, 405–426.
116. Shalabi, A., & Eskander, D. M. (2022). Isolation of secondary metabolites from marine Streptomyces sparsus ASD203 and evaluation its bioactivity. *Egyptian Journal of Chemistry, 65*(3), 539–547.
117. Sherif, M. H., Hussein, M. M., Eid, R. S., & Abas, A.-S. M. (2019). Biochemical study on the effect of morin and rutin in amelioration of titanium dioxide nanoparticle toxicity in rat liver. *Biochemistry Letters, 15*(1), 167–185.
118. Shi, F., Zhao, J.-H., Liu, Y., Wang, Z., Zhang, Y.-T., & Feng, N.-P. (2012). Preparation and characterization of solid lipid nanoparticles loaded with frankincense and myrrh oil. *International journal of nanomedicine*, 2033–2043.
119. Shin, T. H., Seo, C., Lee, D. Y., Ji, M., Manavalan, B., Basith, S., Chakkarapani, S. K., Kang, S. H., Lee, G., & Paik, M. J. (2019). Silica-coated magnetic nanoparticles induce glucose metabolic dysfunction in vitro via the generation of reactive oxygen species. *Archives of toxicology, 93*, 1201–1212.
120. Sinha, A. K. (1972). Colorimetric assay of catalase. *Analytical biochemistry, 47*(2), 389–394.
121. Sliai, A. M. (2015). Protective effects of wheat germ oil on doxorubicin-induced hepatotoxicity in male mice. *Intern. J. Res. Stud. Bios, 3*, 21–25.
122. Soliman, M. G., Ashry, O. M., Ahmed, M. A., & Abd El-Naby, Y. H. (2015). Improvement of hematopoietic and immunologic findings in sublethal gamma irradiated rats treated with bone marrow transplantation and wheat germ oil. *Journal of Immune Based Therapies, Vaccines and Antimicrobials, 4*(2), 9–18.
123. Souto, E. B., Doktorovova, S., Zielinska, A., & Silva, A. M. (2019). Key production parameters for the development of solid lipid nanoparticles by high shear homogenization. *Pharmaceutical development and technology, 24*(9), 1181–1185.
124. Strand, N., Anderson, M. A., Attanti, S., Gill, B., Wie, C., Dawodu, A., Pagan-Rosado, R., Harbell, M. W., & Maloney, J. A. (2024). Diabetic neuropathy: Pathophysiology review. *Current pain and headache reports, 28*(6), 481–487.
125. Suvarna, K. S., Layton, C., & Bancroft, J. D. (2018). *Bancroft's theory and practice of histological techniques E-Book*: Elsevier health sciences.
126. Tamber, S. S., Bansal, P., Sharma, S., Singh, R. B., & Sharma, R. (2023). Biomarkers of liver diseases. *Molecular Biology Reports, 50*(9), 7815–7823.

127. Tappel, A., & Zalkin, H. (1959). Inhibition of lipide peroxidation in mitochondria by vitamin E. *Archives of Biochemistry and Biophysics, 80*(2), 333–336.

128. Taş, A., Çakmak, N. K., Agbektaş, T., Zontul, C., Özmen, E., & Siliğ, Y. (2020). Determination of the impacts of titanium dioxide nanoparticles on a number of xenobiotic-metabolizing enzymes in rat liver. *Scientific Journal of Mehmet Akif Ersoy University, 3*(3), 77–83.

129. Tripathi, N., & Jialal, I. (2020). Conjugated hyperbilirubinemia.

130. Vasantharaja, D., Ramalingam, V., & Reddy, G. A. (2015). Oral toxic exposure of titanium dioxide nanoparticles on serum biochemical changes in adult male Wistar rats. *Nanomedicine journal, 2*(1).

131. Vasantharaja, D., Ramalingam, V., Thangapandiyan, S., Sridhar, N., & Reddy, G. D. (2019). TiO2 nanoparticles induced oxidative stress mediated DNA damage in the liver of adult male Wistar rats. *Advanced Materials Letters, 10*(2), 145–150.

132. Viegas, C., Patrício, A. B., Prata, J. M., Nadhman, A., Chintamaneni, P. K., & Fonte, P. (2023). Solid lipid nanoparticles vs. nanostructured lipid carriers: a comparative review. *Pharmaceutics, 15*(6), 1593.

133. Vijayabaskar, G., & Elango, V. (2018). Determination of phytocompounds in Withania somnifera and Smilax china using GC-MS technique. *J Pharmacogn Phytochem, 7*(6), 554–557.

134. Wang, Y., Jin, J., Wu, G., Wei, W., Jin, Q., & Wang, X. (2025). Omega-9 monounsaturated fatty acids: a review of current scientific evidence of sources, metabolism, benefits, recommended intake, and edible safety. *Critical Reviews in Food Science and Nutrition, 65*(10), 1857–1877.

135. Wani, M. R., Maheshwari, N., & Shadab, G. (2021). Eugenol attenuates TiO 2 nanoparticles-induced oxidative damage, biochemical toxicity and DNA damage in Wistar rats: an in vivo study. *Environmental Science and Pollution Research, 28*, 22664–22678.

136. Weissman, M., & Klein, B. (1958). Evaluation of glucose determinations in untreated serum samples. *Clinical chemistry, 4*(5), 420–422.

137. Williams Jr, C. H., & Kamin, H. (1962). Microsomal triphosphopyridine nucleotide-cytochrome c reductase of liver. *Journal of biological Chemistry, 237*(2), 587–595.

138. Wu, B., Ootani, A., Iwakiri, R., Sakata, Y., Fujise, T., Amemori, S., Yokoyama, F., Tsunada, S., Toda, S., & Fujimoto, K. (2006). T cell deficiency leads to liver carcinogenesis in Azoxymethane-treated rats. *Experimental Biology and Medicine, 231*(1), 91–98.

139. Wu, F., Tian, F., Jin, Z., Liu, J., Jin, W., Chen, X., Wang, Z., Jia, X., Liu, B., & Liu, L. (2022). Antioxidant capacities of heat-treated wheat germ and extruded compounded bran. *Cereal Chemistry, 99*(3), 582–592.

140. Yang, J.-G., He, X.-F., Huang, B., Zhang, H.-A., & He, Y.-K. (2018). Rule of changes in serum GGT levels and GGT/ALT and AST/ALT ratios in primary hepatic carcinoma patients with different AFP levels. *Cancer biomarkers, 21*(4), 743–746.

141. Younes, N. R. B., Amara, S., Mrad, I., Ben-Slama, I., Jeljeli, M., Omri, K., El Ghoul, J., El Mir, L., Rhouma, K. B., & Abdelmelek, H. (2015). Subacute toxicity of titanium dioxide (TiO 2) nanoparticles in male rats: emotional behavior and pathophysiological examination. *Environmental Science and Pollution Research, 22*, 8728–8737.

142. Zargar, S., Wani, T. A., & Rizwan Ahamad, S. (2023). An insight into wheat germ oil nutrition, identification of its bioactive constituents and computer-aided multidimensional data analysis of its potential anti-inflammatory effect via molecular connections. *Life, 13*(2), 526.
143. Zaveri, M. (2021). Bioactivity of Dodecanoic Acid Extracted from Geitlerinema sp. TRV57. *Indian Journal of Pharmaceutical Education & Research, 55*(1).
144. Zhang, B., Ramesh, G., Norbury, C., & Reeves, W. (2007). Cisplatin-induced nephrotoxicity is mediated by tumor necrosis factor-α produced by renal parenchymal cells. *Kidney international, 72*(1), 37–44.
145. Zhang, W., Sun, J., Liu, F., Li, S., Wang, X., Su, L., & Liu, G. (2024). Alleviative effect of lactoferrin interventions against the hepatotoxicity induced by titanium dioxide nanoparticles. *Biological Trace Element Research, 202*(2), 624–642.
146. Zhu, J.-G., Cheng, B.-C., Lee, W.-C., Li, L.-C., Lee, C.-H., Long, G., & Chen, J.-B. (2016). Serum alkaline phosphatase levels are not associated with increased death risk in prevalent hemodialysis patients: 5-year experience in a single hemodialysis center. *Kidney and Blood Pressure Research, 41*(4), 498–506.
147. Zhu, S., Jiao, W., Xu, Y., Hou, L., Li, H., Shao, J., Zhang, X., Wang, R., & Kong, D. (2021). Palmitic acid inhibits prostate cancer cell proliferation and metastasis by suppressing the PI3K/Akt pathway. *Life Sciences, 286*, 120046.

Figures

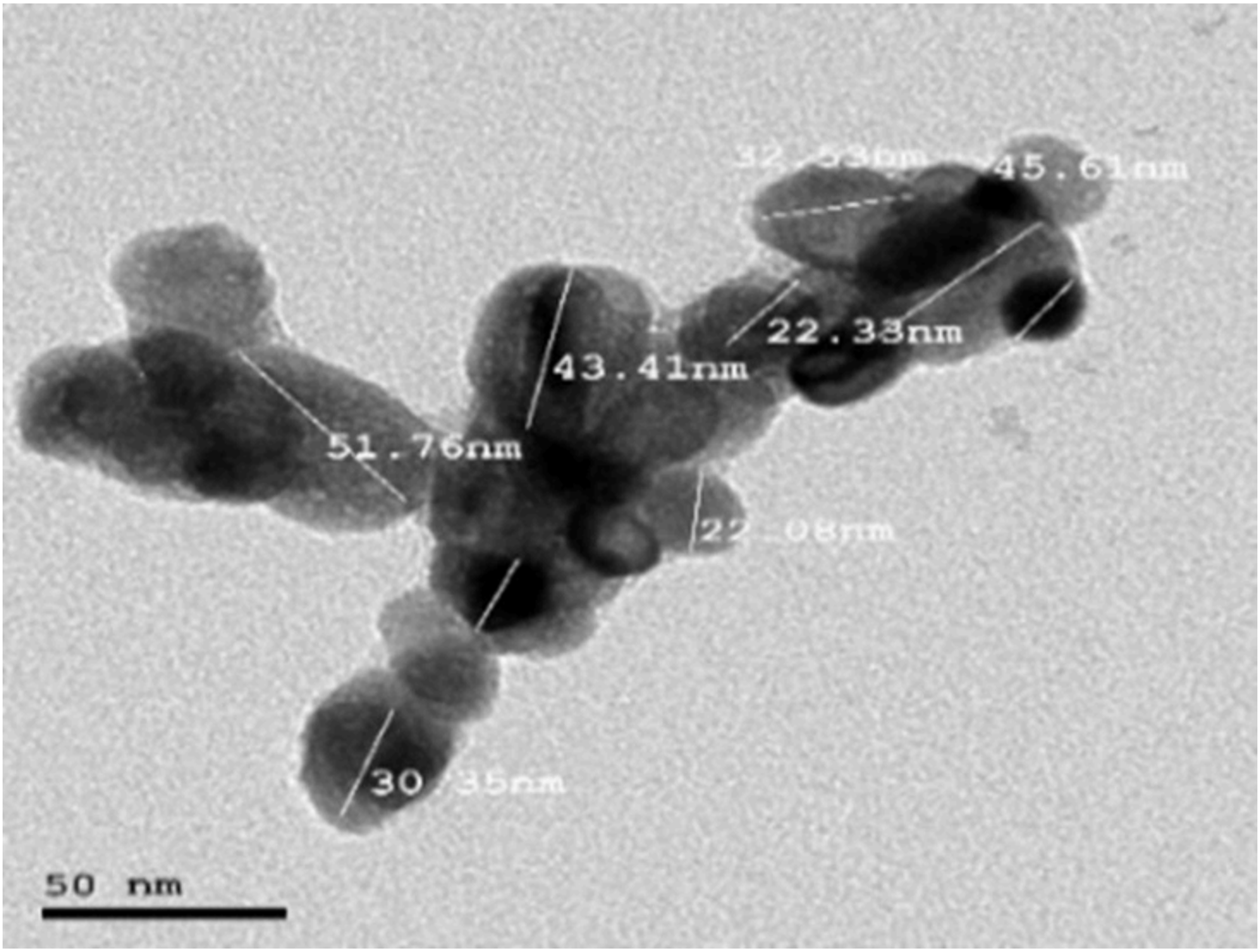


Figure 1

Transmission electron microscope of TiO_2 NPs

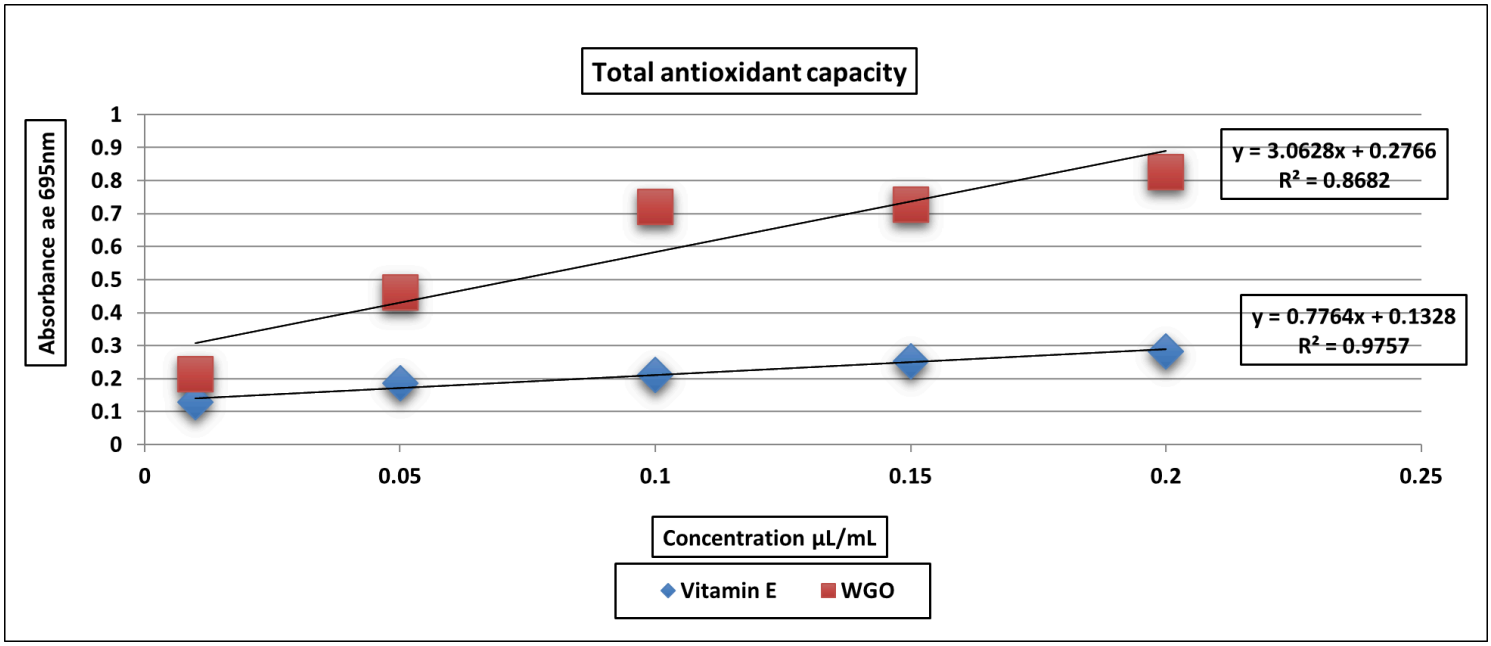


Figure 2

Total antioxidant capacity of WGO and vitamin E by phosphomolybdenum assay

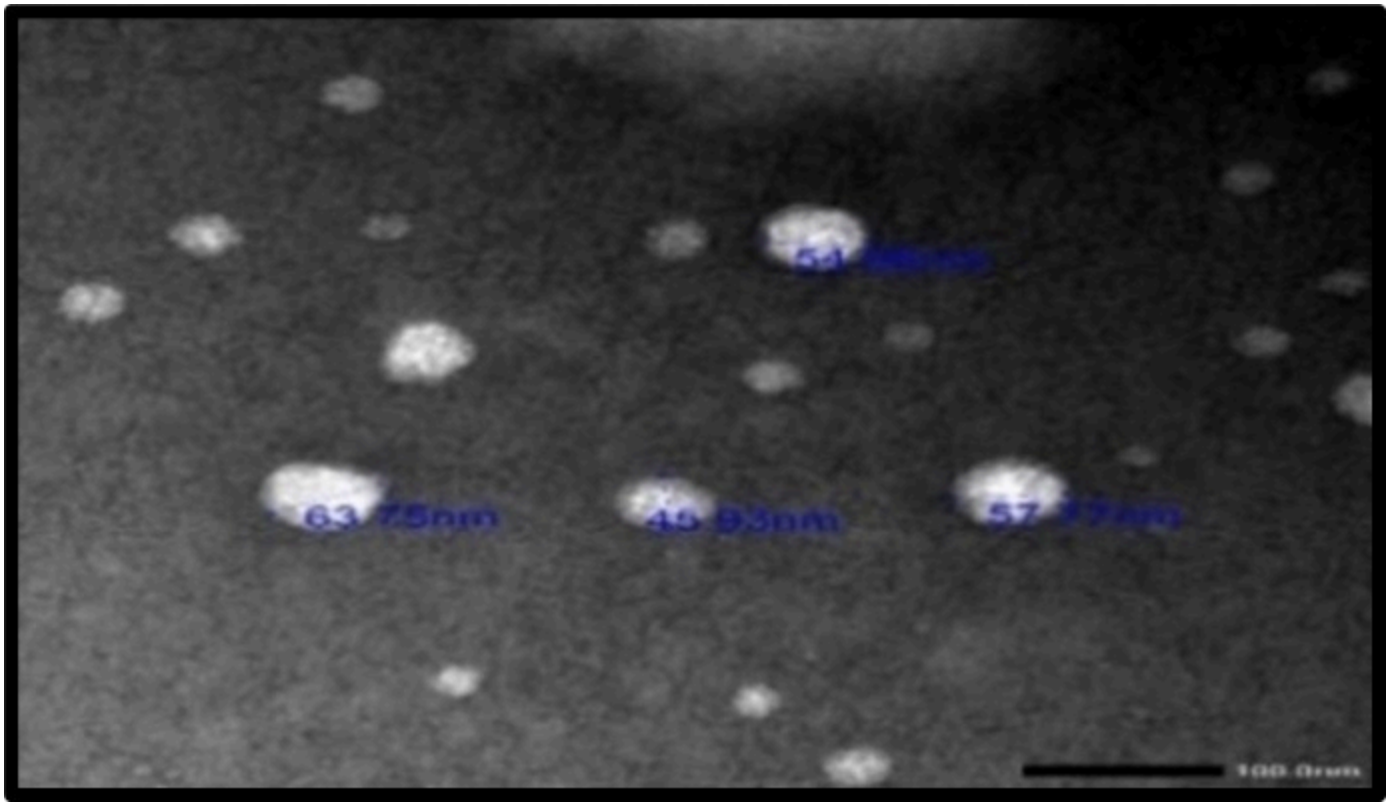


Figure 3

Transmission electron microscope of WGO NLCs

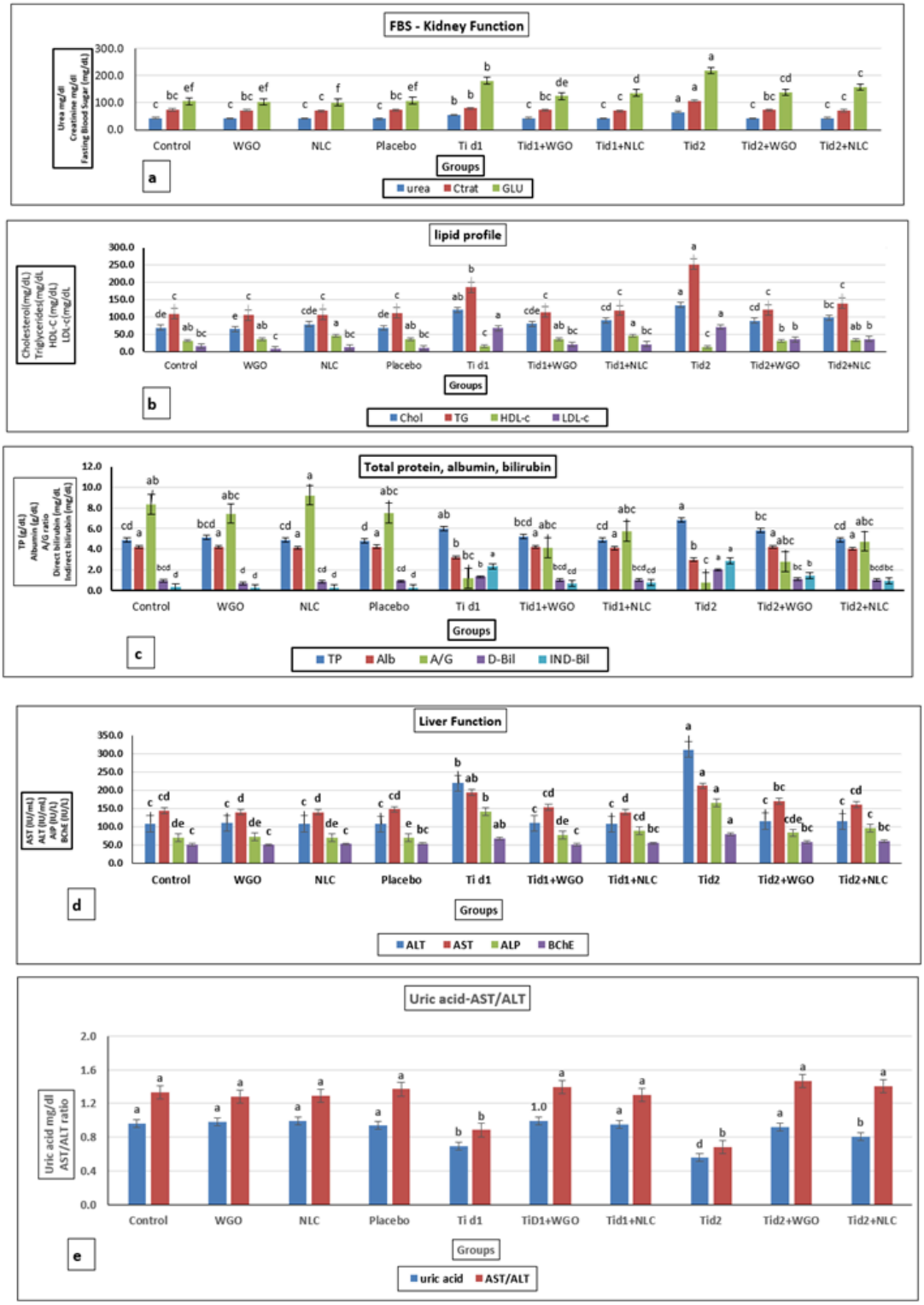


Figure 4

Effects of wheat germ oil and its Nano-formulation on the titanium dioxide nanoparticles induced toxicity on biochemical analysis in blood serum of male rats

The results expressed as (Mean ± SE,n=6)

Tid1; dose 1 of titanium dioxide nanoparticles (5mg/Kg body weight), Tid2; dose 2 of titanium dioxide nanoparticles (25mg/Kg body weight), WGO; dose of wheat germ oil (270mg/Kg body weight), NLC; dose of wheat germ oil loaded nanostructured lipid carrier (270mg/Kg body weight), Placebo; blank of NLC.

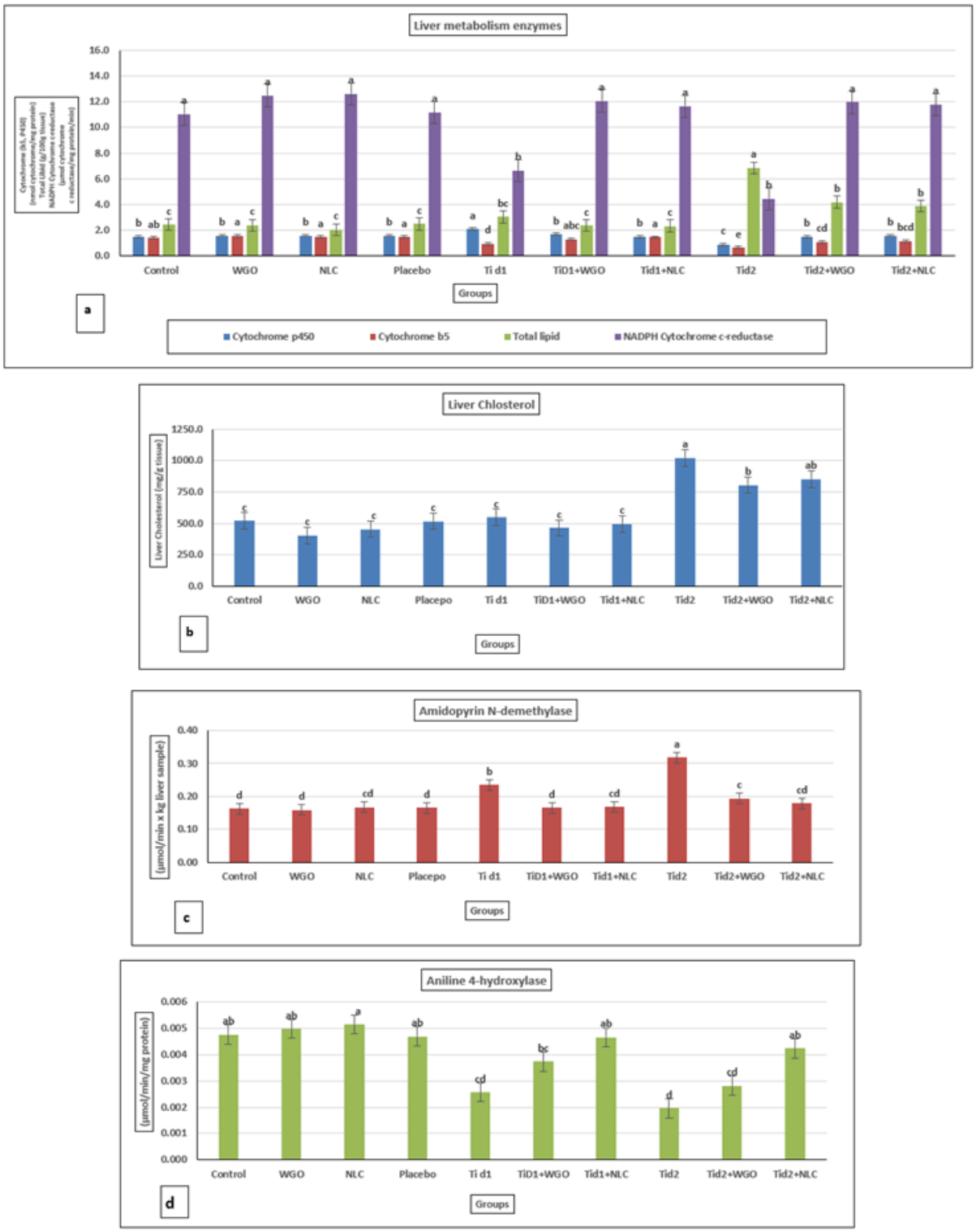


Figure 5

Effects of wheat germ oil and its Nano-formulation on the titanium dioxide nanoparticles induced toxicity on cytochrome b5, cytochrome P450 total lipids NADPH cytochrome c-reductase (a). cholesterol (b),

aminopyrine N-demethylase (c) and aniline 4-hydroxylase (d) in liver homogenate of male rats

The results expressed as (Mean ± SE,n=6)

Tid1; dose 1 of titanium dioxide nanoparticles (5mg/Kg body weight), Tid2; dose 2 of titanium dioxide nanoparticles (25mg/Kg body weight), WGO; dose of wheat germ oil (270mg/Kg body weight), NLC; dose of wheat germ oil loaded nanostructured lipid carrier (270mg/Kg body weight), Placebo; blank of NLC.

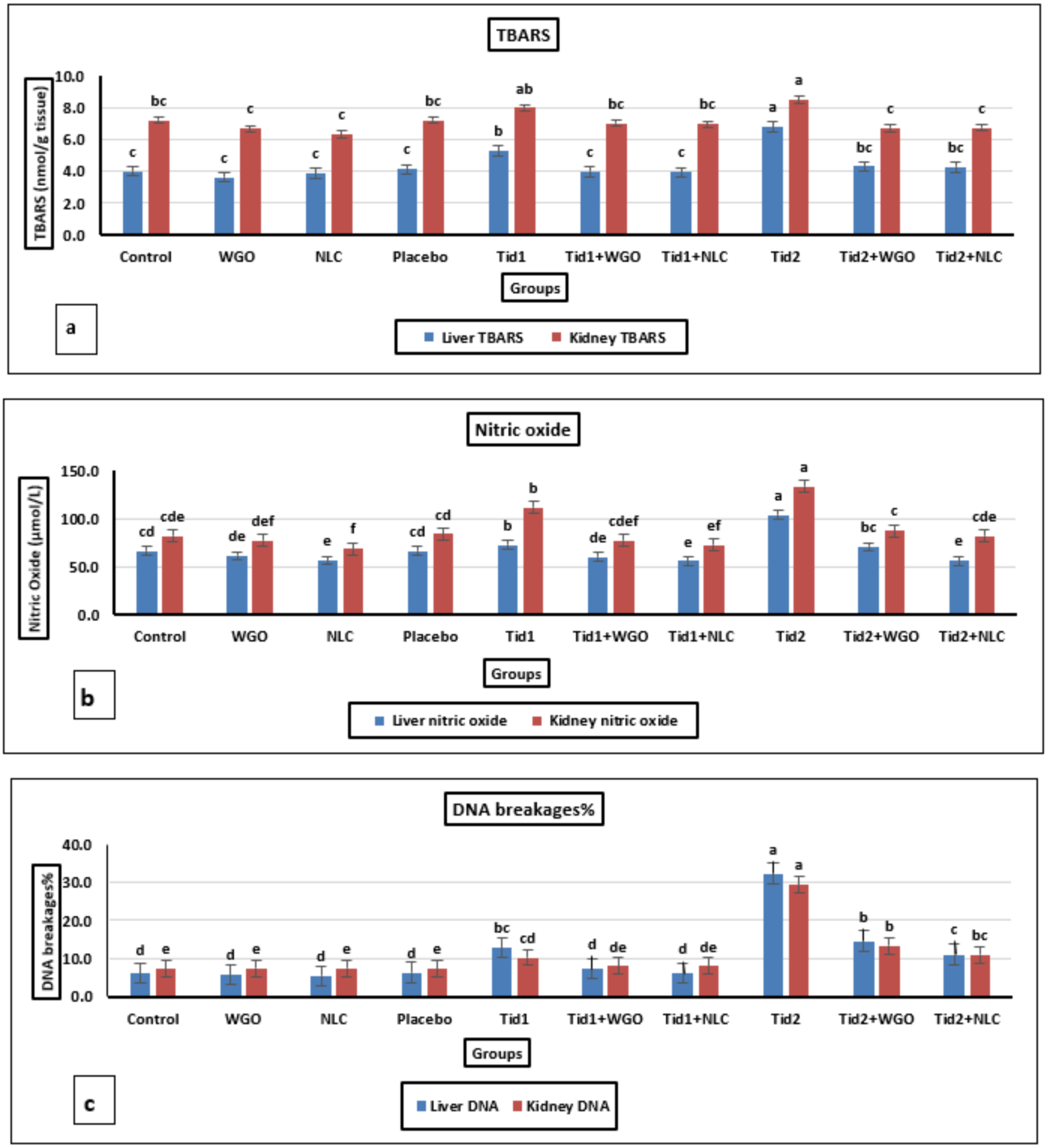
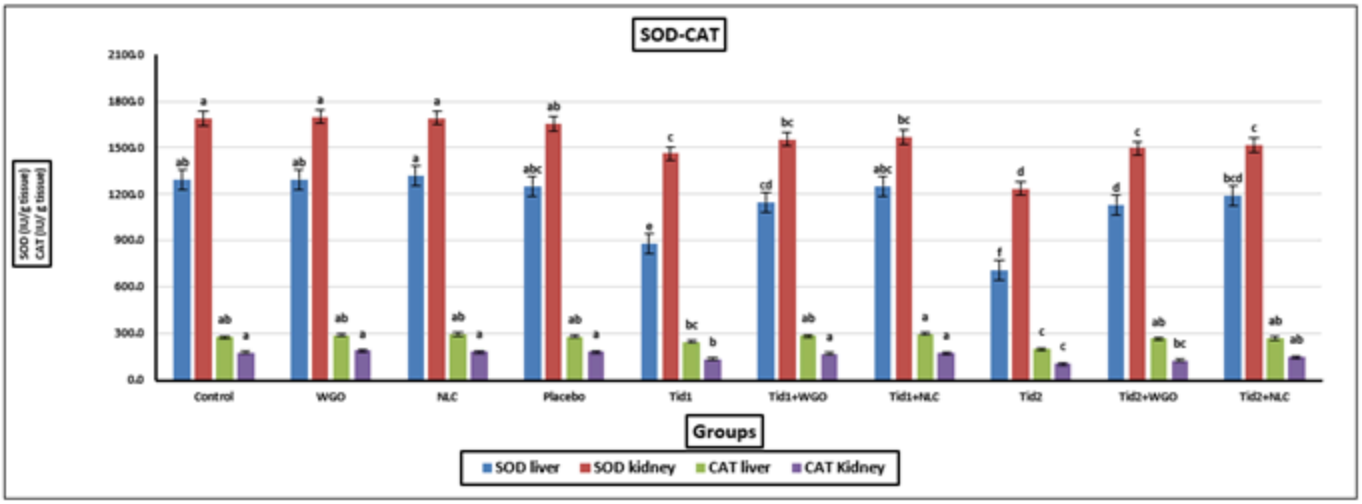


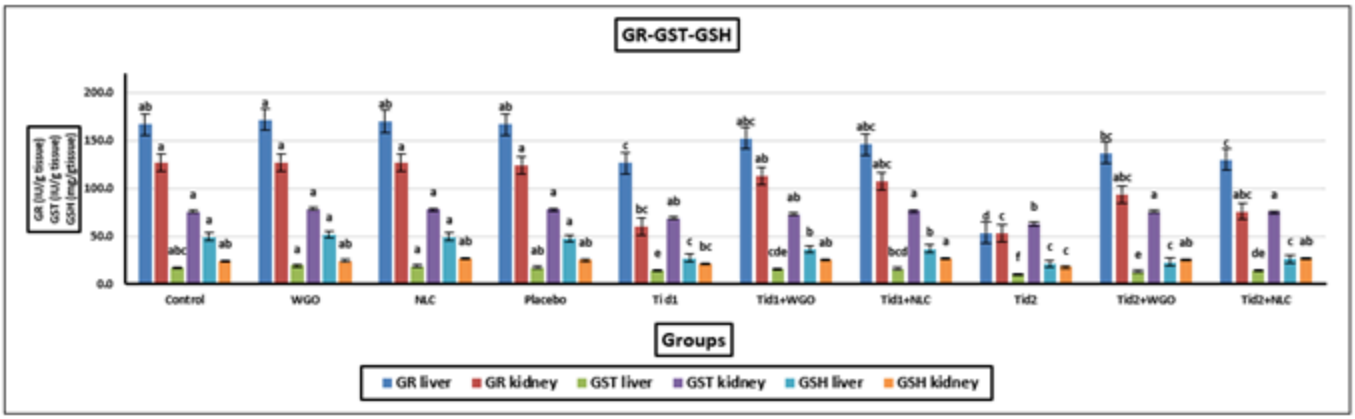
Figure 6

Effects of wheat germ oil and its Nano-formulation on the titanium dioxide nanoparticles induced toxicity on thiobarbituric acid reactive substances (TBARS), DNA breakages and nitric oxide level in liver and kidney homogenate of male rats

The results expressed as (Mean ± SE,n=6)

Tid1; dose 1 of titanium dioxide nanoparticles (5mg/Kg body weight), Tid2; dose 2 of titanium dioxide nanoparticles (25mg/Kg body weight), WGO; dose of wheat germ oil (270mg/Kg body weight), NLC; dose of wheat germ oil loaded nanostructured lipid carrier (270mg/Kg body weight), Placebo; blank of NLC.





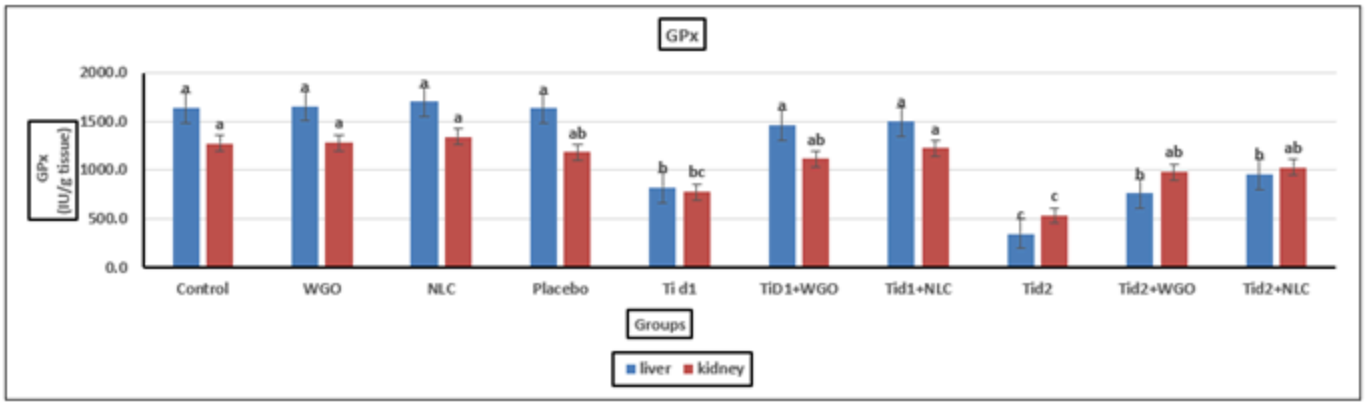


Figure 7

Effects of wheat germ oil and its Nano-formulation on the titanium dioxide nanoparticles induced toxicity on antioxidants enzymes in liver and kidney homogenates of male rats

The results expressed as (Mean ± SE,n=6)

Tid1; dose 1 of titanium dioxide nanoparticles (5mg/Kg body weight), Tid2; dose 2 of titanium dioxide nanoparticles (25mg/Kg body weight), WGO; dose of wheat germ oil (270mg/Kg body weight), NLC; dose of wheat germ oil loaded nanostructured lipid carrier (270mg/Kg body weight), Placebo; blank of NLC

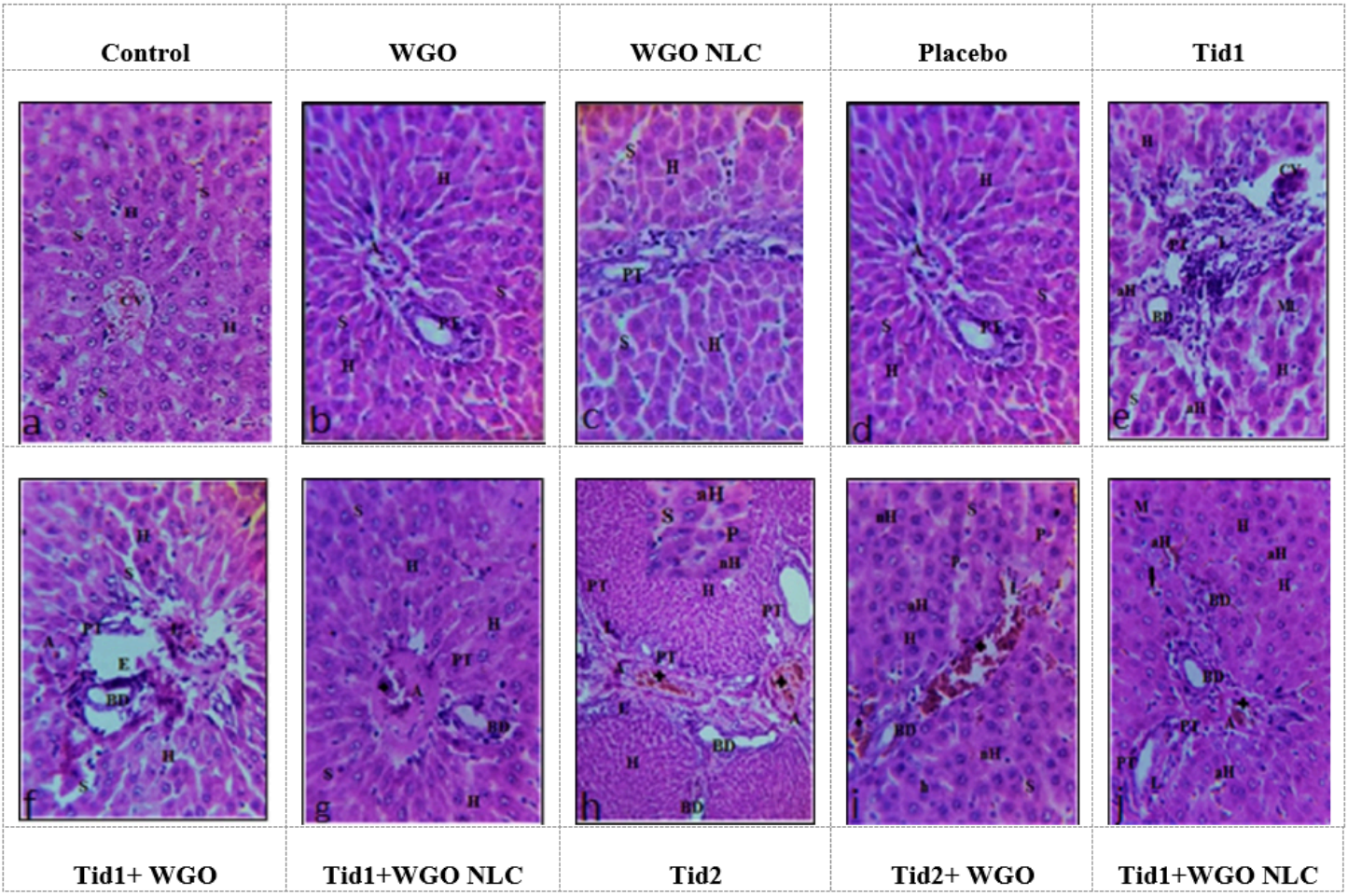


Figure 8

LM Micrograph rats' liver paraffin sections stained by H&E(X400), (a-d) Control group: untreated group, WGO, WGO NLC and placebo, showing normal hepatic architectures of liver tissues, the hepatocytes (H) radiated at central vein and portal tract (PT), a narrow sinusoid (S) and Artery (A). (e) rats' liver treated with Tid1 showing lobular infiltrate by leukocytes and inflammatory cells (L), disarrayed hepatocytes have hyperchromatic nuclei (H) and other vacuolated nuclei (aH) with light basophilic cytoplasm and wide sinusoid (S). A marked dilatation in the portal tract (PT) and bile duct (BD) was seen. (f) Rats treated with Tid1+ WGO showing re-arrangement of hepatocytes surrounding dilatated portal tract (PT), few infiltrating leukocytes and cubiodal epithelial bile duct, the hepatocytes appeared small, rounded nuclei and prominent nucleoli and homogenous cytoplasm. (g) Rats treated with Tid1+ WGO NLC

showing a well recovering of the hepatic tissue, decreased of infiltrating leukocytes at portal tract and organized bile duct, the artery (A) was large and has few deposits of Ti in its lumen (*), the hepatocytes were radiated array at portal tract, have rounded nuclei and homogenous activities cytoplasm and narrow sinusoid (S). (h) rats' liver sections treated Tid2 showing marked degeneration of liver tissue, high proliferating and crowded hepatocytes associated to the adjacent three portal tracts forming liver fibrosis (PT) and infiltrating leukocytes (L), the hepatocytes have pyknotic nuclei (P), vacuolar nuclei (aH) and small dark nuclei and necrotic one with homogenous cytoplasm and narrow sinusoids was seen. A marked dilated bile duct (BD) the artery has a deposit of precipitated Ti in its lumen (*). (i) Tid2 +WGO showing mild regeneration of hepatic tissue, the dilatation in the portal tract with Ti deposit (*), infiltrating few leukocyte (L), many hepatocytes have small, rounded dark nuclei, a prominent nucleolus, a few pyknotic nucle (P) and necrotic one (nH) with homogenous cytoplasm. (j) Rats treated with Tid2 +WGO NLC showing reorganized hepatocytes surrounding the portal tract have few vacuolar nuclei (aH), few mitotic (M) and many healthy hepatocytes.

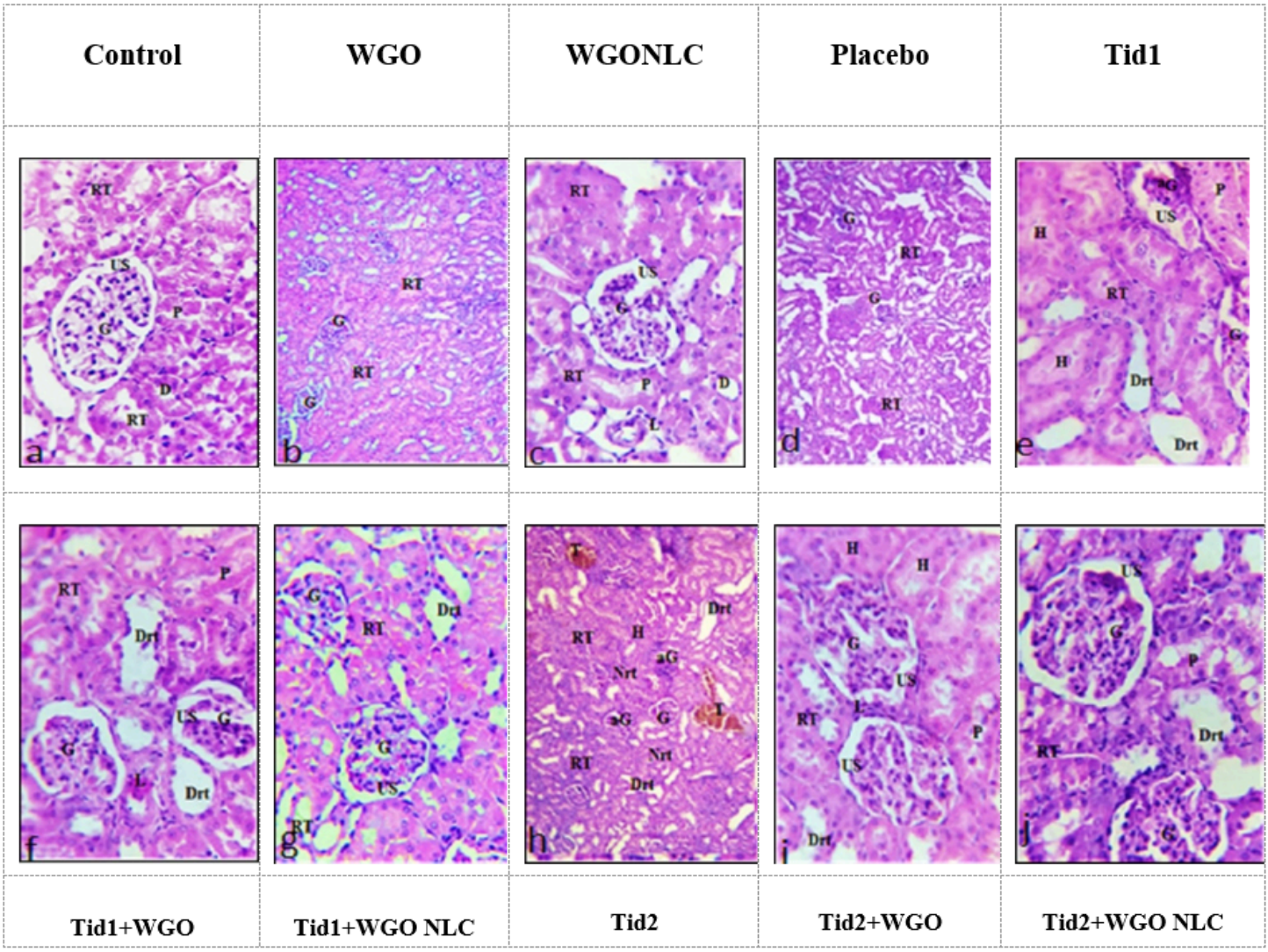


Figure 9

LM photomicrograph of rats' kidney cortex paraffin sections stained by H&E(X400), (a –d) control groups: Untreated group, WGO, WGO NLC and placebo group showing normal renal glomeruli with normal urinary space and normal renal tubules with tubular epithelium of proximal tubules and distal tubules, and few infiltrating lymphocytes in the interstitial tissue. (e) Group Tid1 showing degeneration of the kidney cortex, as atrophy glomeruli increased the urinary space, disorganzed kidney tubules, many hyalinized proximal tubules; and many dilated renal tubules lumen. (f) Group Tid1 + WGO showing recovery of the kidney tissues appeared as organized glomeruli with narrow urinary space and many mesangial cells, an improved renal tubule, many organized proximal tubules and mild dilated lumen. (g) Group Tid1 + WGO NLC showing reorganization of the kidney tissue as improvement of renal tubules, a few dilated renal tubules and organized glomeruli. (h) Group Tid2 showing marked degenerative kidney tissue, appeared as precipitation of Ti in the interstial tissue, many atrophic glomeruli with reduction of masengal cell and widening of the urinary space, a crowded and dilated renal tubule, many with necrotic tubular epithelial cell and hyaline lumen. (i) Rats treated with Tid2+WGO showed an improvement in kidney tissue, was showing reorganized of glomureli with dark nuclei masengal cell with narrow urinary space and epithelial cells of the renal tubule with few hyaline tubular lumens. (j) Group Tid2+WGO NLC showing an organized glomerulus, an improvement of most renal tubules with mild dilations of tubular lumen and absent of hyaline castes of lumen, Glomeruli (G); urinary space (US); Atrophy glomeruli (aG), Renal tubules (RT), Dilated renal tubules (Drt); Necrotic renal tubules (Nrt); Distal tubules (D); Proximal tubules (P): Hyalinized proximal tubules (H); lymphocytes(L).

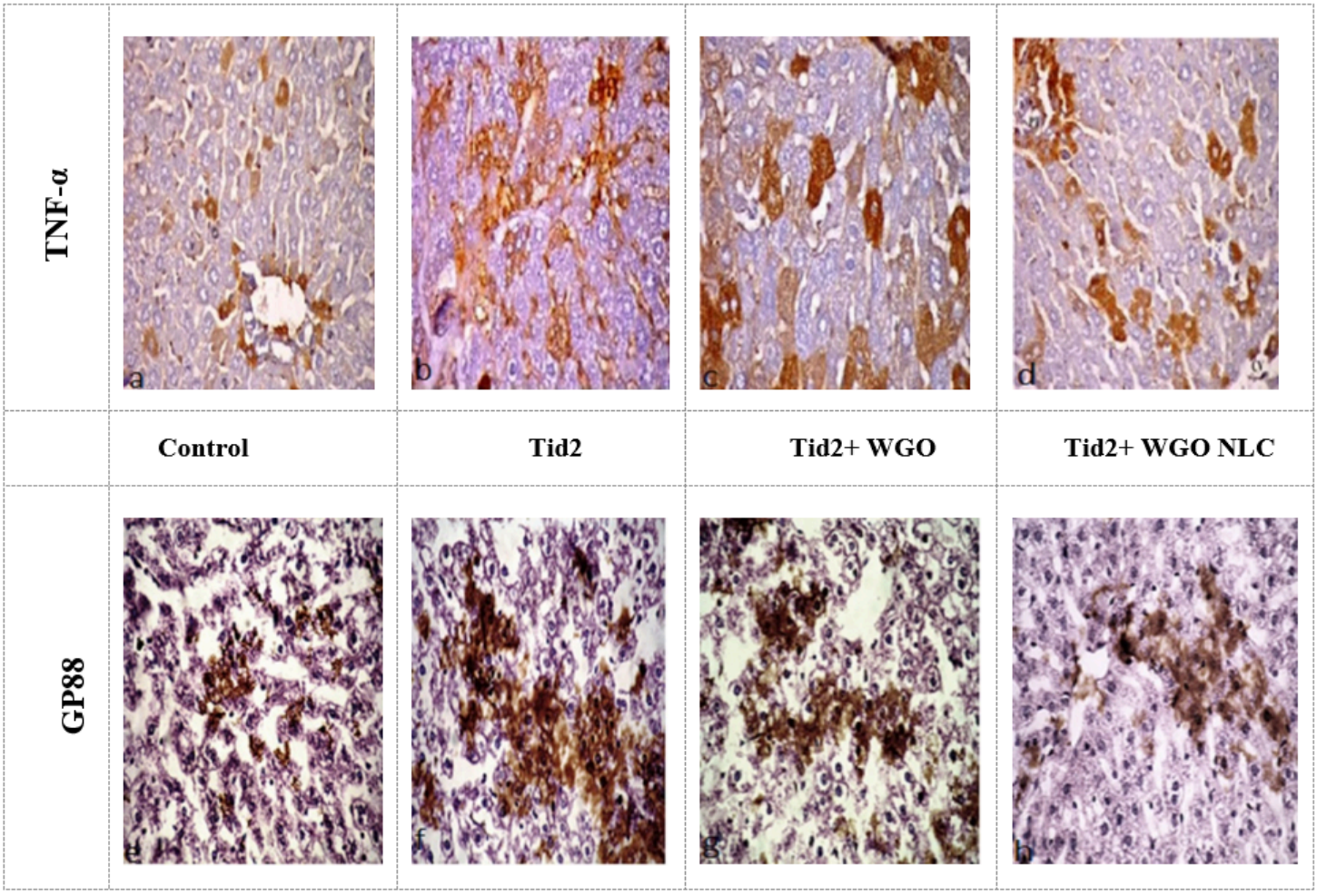


Figure 10

Paraffin section microphotograph of rat liver tissue, illustrate the immunostaining of TNF-a (a-d) and GP88 (e-h). control group (a) showing weak immunoexpression of TNF-α in hepatocytes appeared as small granules in few cells around the portal tract. Group received Tid2 (b) showing strong positive(ve3+) immunoexpression of TNF-α in most hepatocytes cytoplasm as brown coarse granules around the portal tract and central vein, a moderate positive expression of TNF-α (most endothelial cell at sinusoid (S). Group received (Tid2+ WGO) (c) showing moderate TNF-α immunoexpression (ve2+) in some hepatocytes as a tinny brown granule. Group received (Tid2+ WGO NLC) (d) showing a decreased immunoexpression of TNF-α in few degenerative hepatocytes **(TNF+ABC, X400).** Control rat liver, (e) showing an immunoexpression of GP88 protein as brown color in few degenerative hepatocytes cytoplasm at the portal tract region, a blue negative color of the hepatocytes nuclei. Group received Tid2 (f) showing strong positive immunoexpression of GP88 protein(ve3+) in area of degenerative hepatocytes cytoplasm between two adjust portal tract. group received (Tid2+ WGO) (g) showing moderate positive expression of GP88 protein(ve2+) in area of degenerative hepatocytes cytoplasm upper the nuclei appeared as diffuse brown color adjust to the portal tract. Group received (Tid2+ WGO NLC) (h) showing weak positive immunoexpression of GP88 protein in area of degenerative hepatocytes cytoplasm around the portal tract, **(GP88 +DAB satin, X400 Mag).**

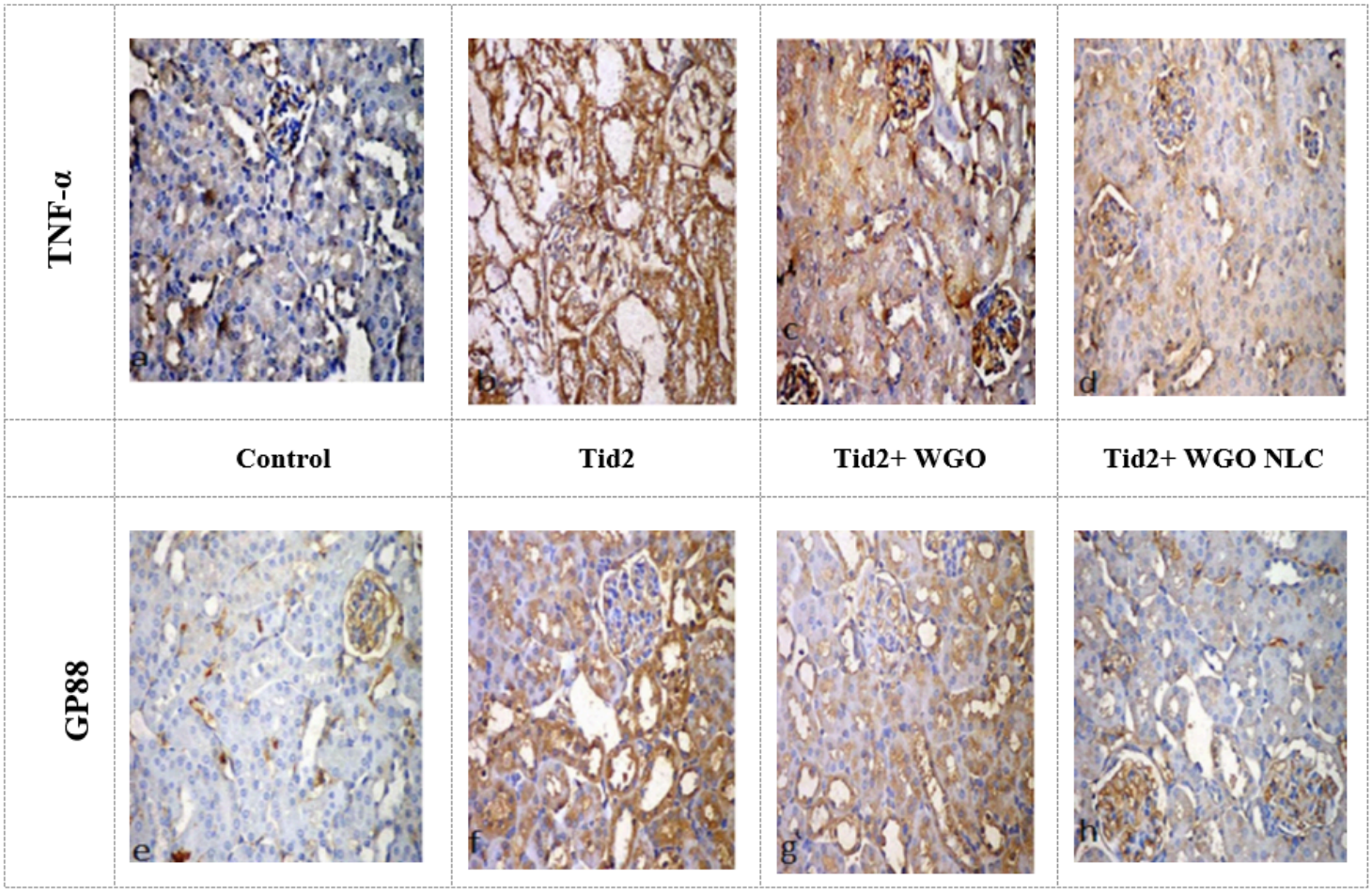


Figure 11

Paraffin section microphotograph of rat kidney illustrate the immunostaining of TNF-a (a-d) and GP88(e-h) in kidney cortex. A control rat kidney (a) showing weak brown granules of positive TNF-α expression (ve+) in few renal tubular cytoplasm and mesangial cells of glomeruli with the negative blue color nuclei of control group. Group received (Tid2) (b) showing strong brown granules of positive TNF-α immunoexpression (ve3+) Group received (Tid2+ WGO) (c) showing moderate positive brown granules of TNF-α immunoexpression (ve2+) Group received (Tid2+ WGO NLC) (d) showing decreased of TNF-α expression in most renal tubules and glomeruli **(TNF+ABC, X400).** A control rat kidney (e) showing an immunoexpression of GP88 appeared as weak positive (ve+) brown granules in few degenerative renal tubular cells cytoplasm and mesangial cells of glomeruli, a negative reaction was noticed in healthy renal tubules and blue negative nuclei. Group received (Tid2) (f) showing strong immunoexpression of GP88 (ve3+) as dark brown granules in most renal tubular cells and moderate in mesangial cells of glomeruli (ve2+). Group received (Tid2+ WGO) (g) showing moderate positive immunoexpression of GP88 (ve2+) as brown granules in dilated renal tubular cells cytoplasm and weak in mesangial cells of glomeruli (ve+). Group received (Tid2+ WGO NLC) (h) showing a decreased immunoexpression of GP88 (ve+) in few renal tubular cells and most glomeruli **(GP88+ABC satin, X400).**

Supplementary Files

This is a list of supplementary files associated with this preprint. Click to download.

- supplementarydata.docx